

Supporting Information for

Site-specific bioorthogonal labeling for fluorescence imaging of intracellular proteins in living cells

Tao Peng^{†,‡,*} and Howard C. Hang^{‡,*}

[†]School of Chemical Biology and Biotechnology, Peking University Shenzhen Graduate School, Shenzhen 518055, China [‡]Laboratory of Chemical Biology and Microbial Pathogenesis, The Rockefeller University, New York, NY 10065, United States

* hhang@rockefeller.edu

* pengtao@pkusz.edu.cn

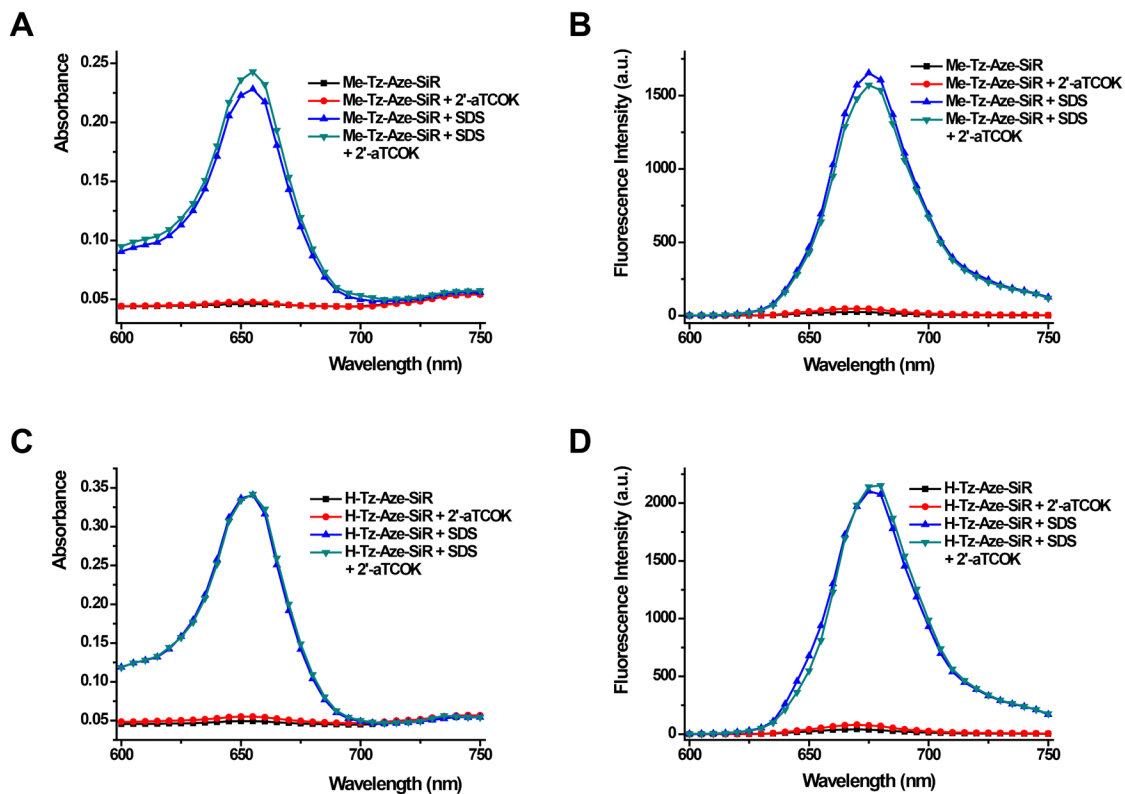
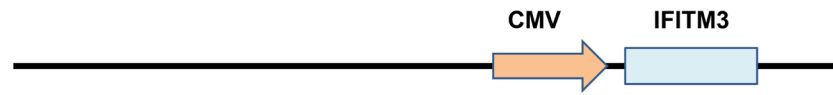
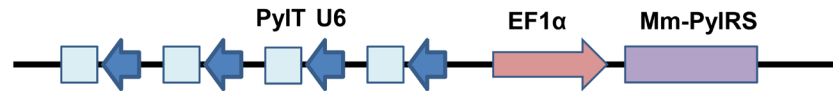


Figure S1. Photophysical characterization of tetrazine derivatives of azetidine-silicon-rhodamines (Aze-SiR). Absorption (A and C) and fluorescence (B and D) spectra of Me-Tz-Aze-SiR (2 μ M; A and B) and H-Tz-Aze-SiR (2 μ M; C and D) before and after reaction with 2'-aTCOK (20 μ M) in phosphate buffer saline (PBS) in the absence or presence of 0.1% SDS. Addition of SDS can dramatically increase both the absorbance (A and C) and fluorescence (B and D) of tetrazine-Aze-SiR.

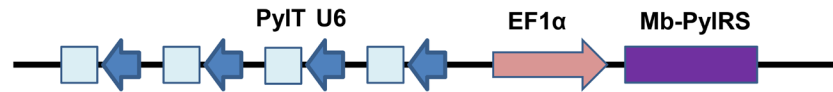
(A) pCMV-HA-IFITM3



(B) pEF1 α -FLAG-Mm-PyIRS



(C) pEF1 α -FLAG-Mb-PyIRS



(D) pCMV-FLAG-Mm-PyIRS

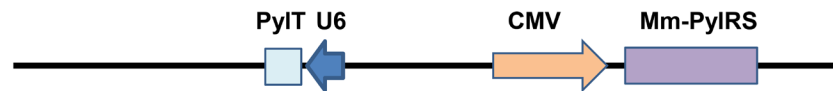


Figure S2. Plasmids used in this study. (A) pCMV-HA-IFITM3, (B) pEF1 α -FLAG-Mm-PyIRS,¹ (C) pEF1 α -FLAG-Mb-PyIRS,² and (D) pCMV-FLAG-Mm-PyIRS.³ The differences between (B) and (D) include the promoter and Pyl-tRNA copy number.

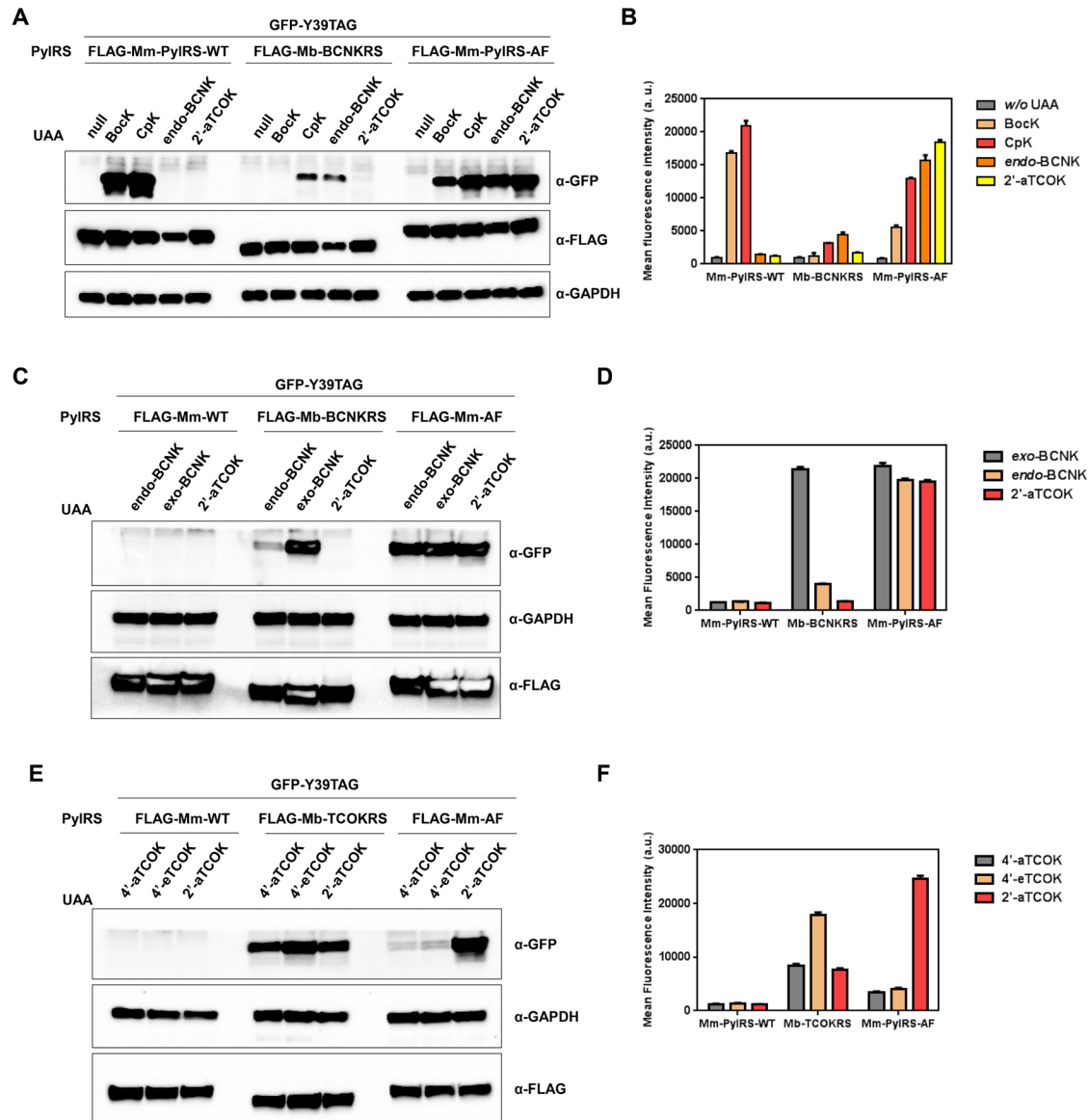


Figure S3. Screening the optimal PyIRS for different unnatural amino acids (UAAs) in the expression of GFP-Y39TAG. Cells were co-transfected with pCMV-GFP-Y39TAG and the indicated PyIRS plasmids in the presence of UAAs (1 mM) for 20 h, and then lysed for Western blotting analysis (A, C, and E) or fixed with 4% formaldehyde for flow cytometry analysis (B, D, and F). Flow cytometry data are shown in mean \pm SD, $n = 3$.

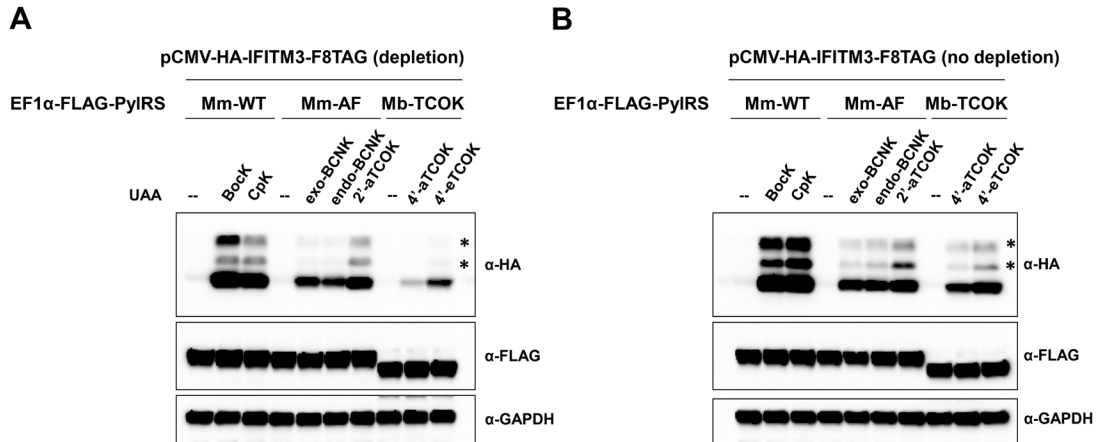


Figure S4. Expression of IFITM3-F8TAG mutant in the presence of different UAAs via genetic code expansion technology. (A) Cells were co-transfected with pCMV-HA-IFITM3-F8TAG and the indicated PyIRS plasmids in the presence of UAAs (50 μ M) for 16 h, depleted with normal media containing no UAAs for 6 h, and then lysed for Western blotting analysis. (B) Cells were co-transfected with pCMV-HA-IFITM3-F8TAG and the indicated PyIRS plasmids in the presence of UAAs (1 mM) for 20 h and then lysed for Western blotting analysis. Higher molecular weight bands in anti-HA blotting marked with asterisks are IFITM3 ubiquitination bands.⁴

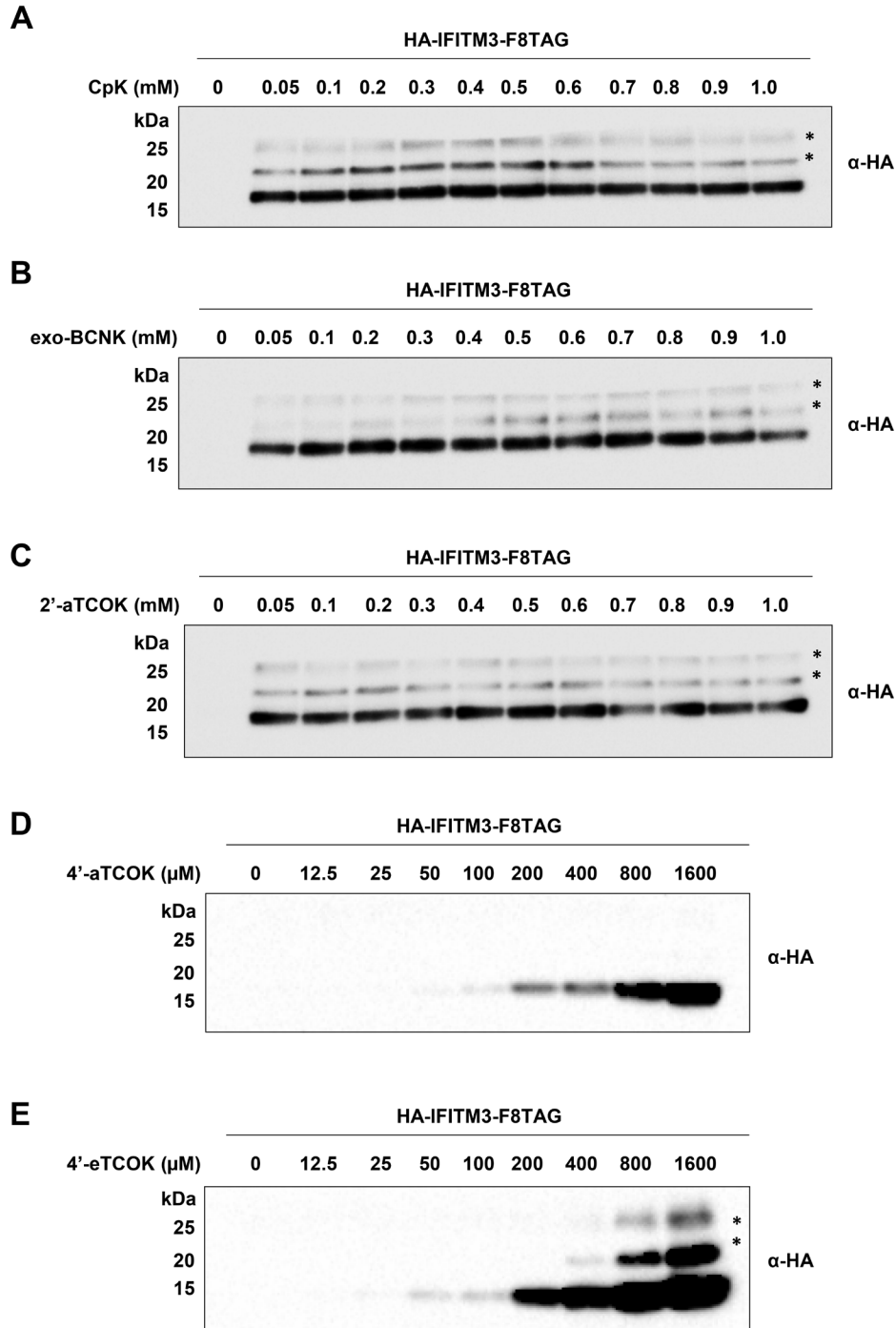


Figure S5. UAA-concentration-dependent expression of HA-IFITM3-F8TAG. Cells were co-transfected with pCMV-HA-IFITM3-F8TAG and pEF1α-FLAG-Mm-PylRS wild-type (for CpK), AF mutant (for exo-BCNK and 2'-aTCOK), or Mb-TCOKRS (for 4'-aTCOK and 4'-eTCOK) plasmids in the presence of varying concentrations of (A) CpK, (B) exo-BCNK, (C) 2'-aTCOK, (D) 4'-aTCOK, or (E) 4'-eTCOK for 20 h, and then lysed for Western blotting analysis. Higher molecular weight bands in anti-HA blotting marked with asterisks are IFITM3 ubiquitination bands.⁴

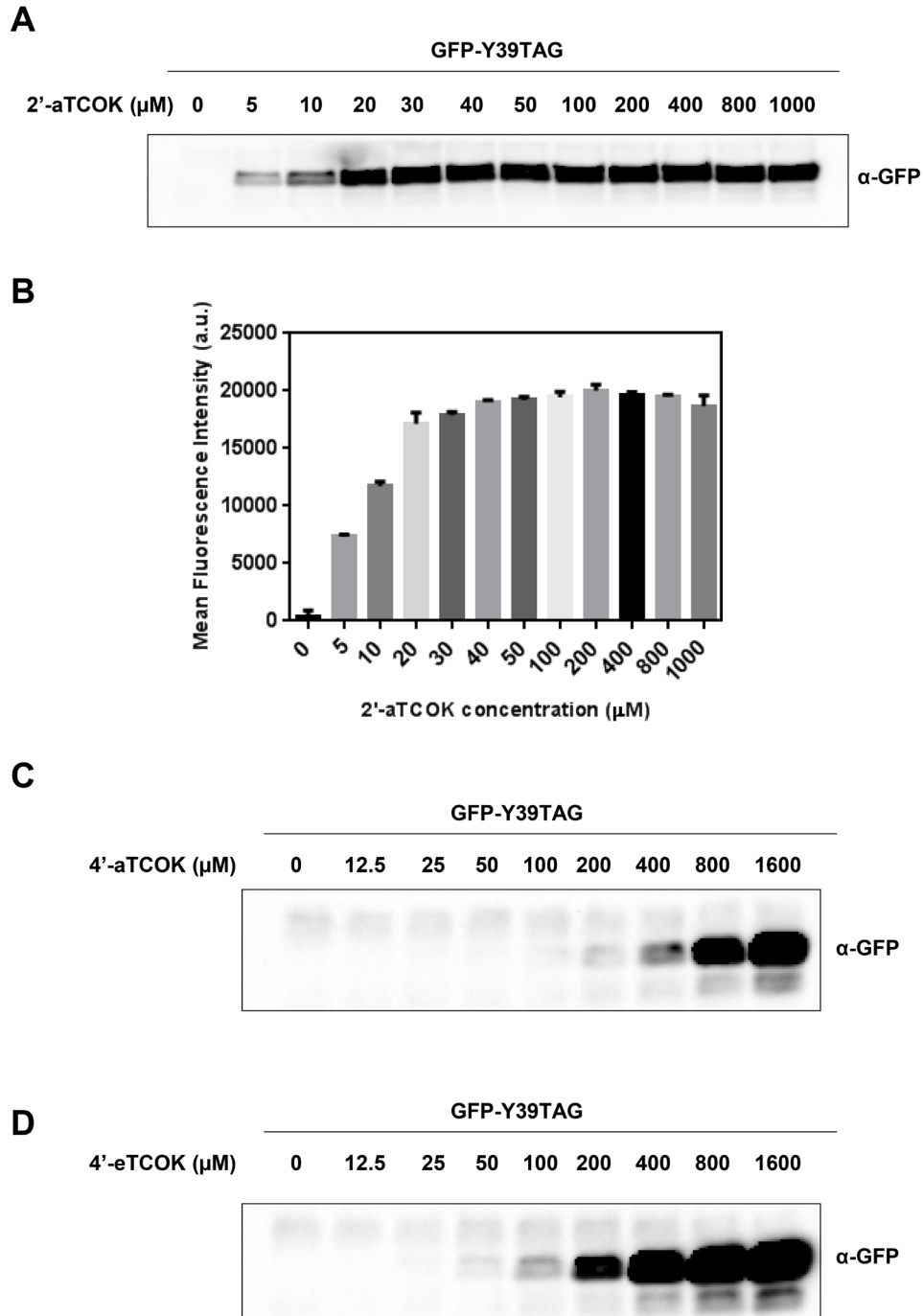


Figure S6. UAA-concentration-dependent expression of GFP-Y39TAG. Cells were co-transfected with pCMV-GFP-Y39TAG and pEF1 α -FLAG-Mm-PyIRS-AF mutant (for 2'-aTCOK) or Mb-TCOKRS (for 4'-aTCOK and 4'-eTCOK) plasmids in the presence of varying concentrations of (A, B) 2'-aTCOK, (C) 4'-aTCOK, or (D) 4'-eTCOK for 20 h, and then lysed for Western blotting (A, C, and D) or flow cytometry (B) analysis. For flow cytometry analysis, three independent experiments were performed. Flow cytometry data are shown in mean \pm SD, $n = 3$.

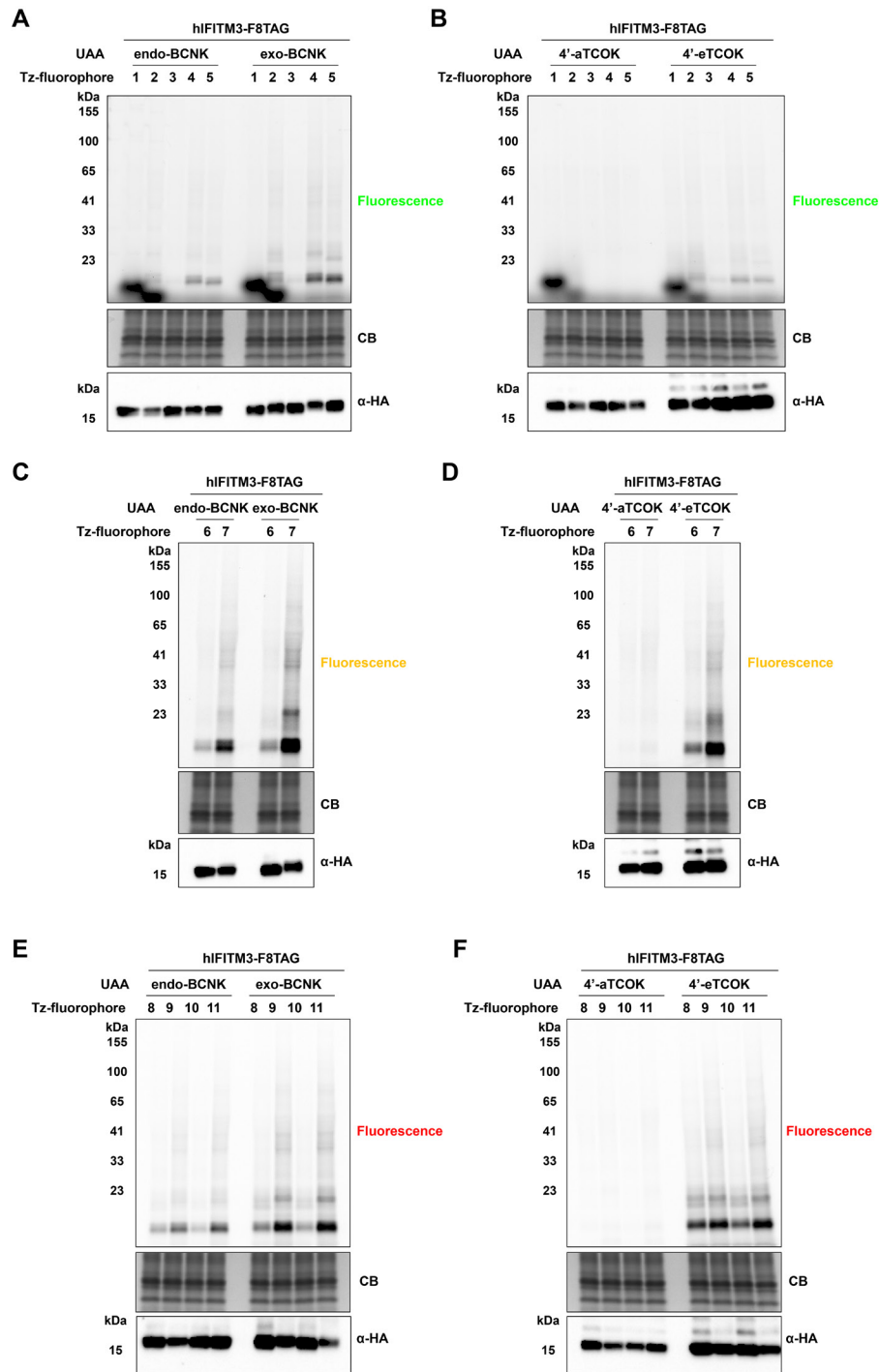


Figure S7. Comparison of BNCK and 4'-TCOK diastereomers for fluorescence labeling of HA-IFITM3-F8TAG in live cells. HeLa cells expressing HA-IFITM3-F8UAA were labeled with (A, B) green tetrazine-fluorophores 1-5, (C, D) orange tetrazine-fluorophores 6-7, or (E, F) red tetrazine-fluorophores 8-11 and lysed for in-gel fluorescence analysis (top panel), Commassie Blue staining (middle panel), and Western blotting analysis (bottom panel) after brief wash. The intense bands in A and B for fluorophores 1 and 2 are from free dyes.

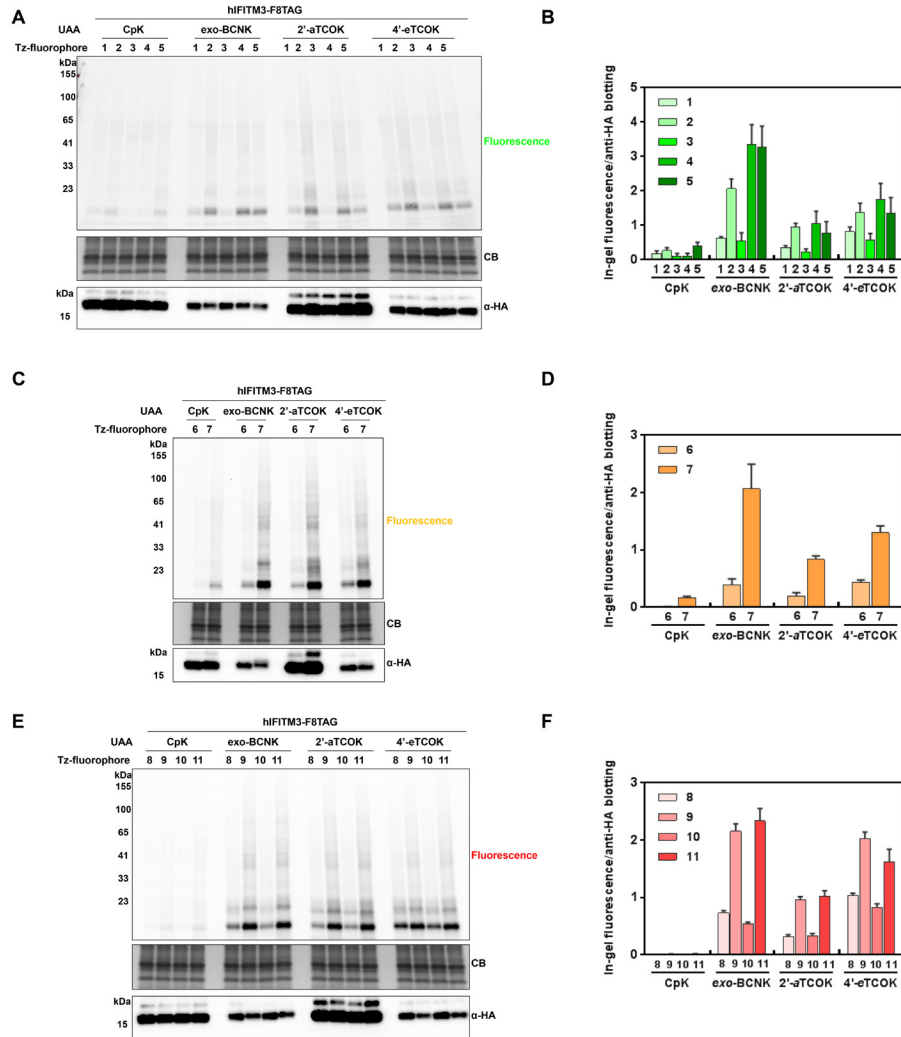


Figure S8. Full gels shown in Figure 3, loading controls (Coomassie Blue staining) for in-gel fluorescence and Western blotting analyses. HeLa cells were co-transfected with HA-IFITM3-F8TAG and Mm-PyIRS-WT (wild-type PyIRS for CpK), Mm-PyIRS-AF (double mutant for exo-BCNK and 2'-aTCOK), or Mb-TCOKRS (TCOKRS for 4'-eTCOK) plasmids in the presence of CpK (50 μ M), exo-BCNK (50 μ M), 2'-aTCOK (50 μ M), or 4'-eTCOK (1 mM) for 16 h and further cultured in complete cell growth medium without UAA for another 6 h. Cells were then labeled with (A) green tetrazine-fluorophores **1-5**, (C) orange tetrazine-fluorophores **6-7**, or (E) red tetrazine-fluorophores **8-11** (500 nM) for 0.5 h, washed for 2 h, and then lysed for in-gel fluorescence, Western blotting, and Coomassie Blue staining. (B, D, and F) Bar graphs showing the fluorescence labeling efficiency of HA-IFITM3-F8UAA with tetrazine-fluorophores relative to the protein expression levels. Intensities of in-gel fluorescence and anti-HA western blotting of every IFITM3 band were quantified, and then the fluorescence intensity was divided by the anti-HA western blotting intensity for each IFITM3 band. Data from three independent replicates were quantified and averaged for plotting the graphs. Data are mean \pm S.E.M., $n = 3$. Representative gels are shown in (A), (C), and (E).

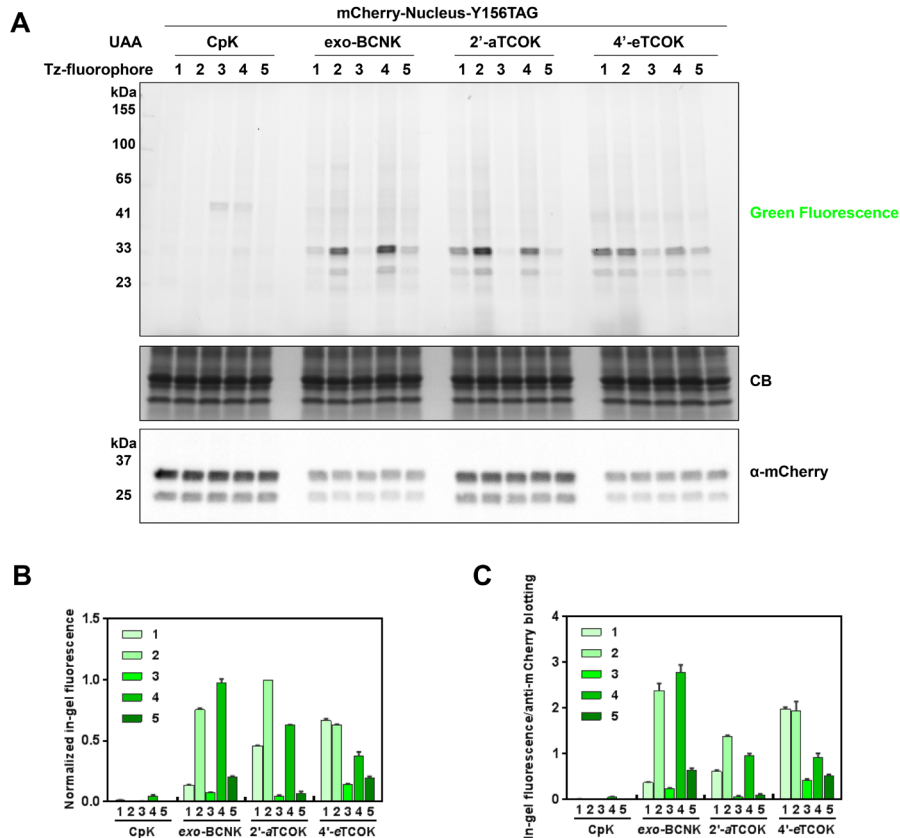


Figure S9. Bioorthogonal fluorescence labeling of mCherry-Nucleus-Y156TAG with green tetrazine-fluorophores. Cells were co-transfected with pmCherry-Nucleus-Y156TAG and Mm-PylRS-WT (wild-type PylRS for CpK), Mm-PylRS-AF (double mutant for exo-BCNK and 2'-aTCOK), or Mb-TCOKRS (TCOKRS for 4'-eTCOK) plasmids in the presence of CpK (50 μ M), exo-BCNK (50 μ M), 2'-aTCOK (50 μ M), or 4'-eTCOK (1 mM) for 16 h and further cultured in complete cell growth medium without UAA for another 6 h. Cells were then labeled with green tetrazine-fluorophores **1-5** for 0.5 h, washed for 2 h, and then lysed for in-gel fluorescence, Coomassie Blue staining, and Western blotting analysis. (A) Representative gels for in-gel fluorescence, Coomassie Blue staining, and Western blotting analysis. (B) Bar graph showing the fluorescence labeling efficiency of mCherry-Nucleus-Y156TAG with tetrazine-fluorophores. Fluorescence intensity of every mCherry-Nucleus band was quantified and normalized to the most intense band of the corresponding gel, the intensity of which is set to 1. Data from three independent replicates were quantified and averaged for plotting the graphs. Data are mean \pm S.E.M., $n = 3$. (C) Bar graph showing the fluorescence labeling efficiency of mCherry-Nucleus with tetrazine-fluorophores relative to the protein expression levels. Intensities of in-gel fluorescence and anti-mCherry western blotting of every mCherry-Nucleus band were quantified, and then the fluorescence intensity was divided by the anti-mCherry western blotting intensity for each mCherry-Nucleus band. Data from three independent replicates were quantified and averaged for plotting the graphs. Data are mean \pm S.E.M., $n = 3$.

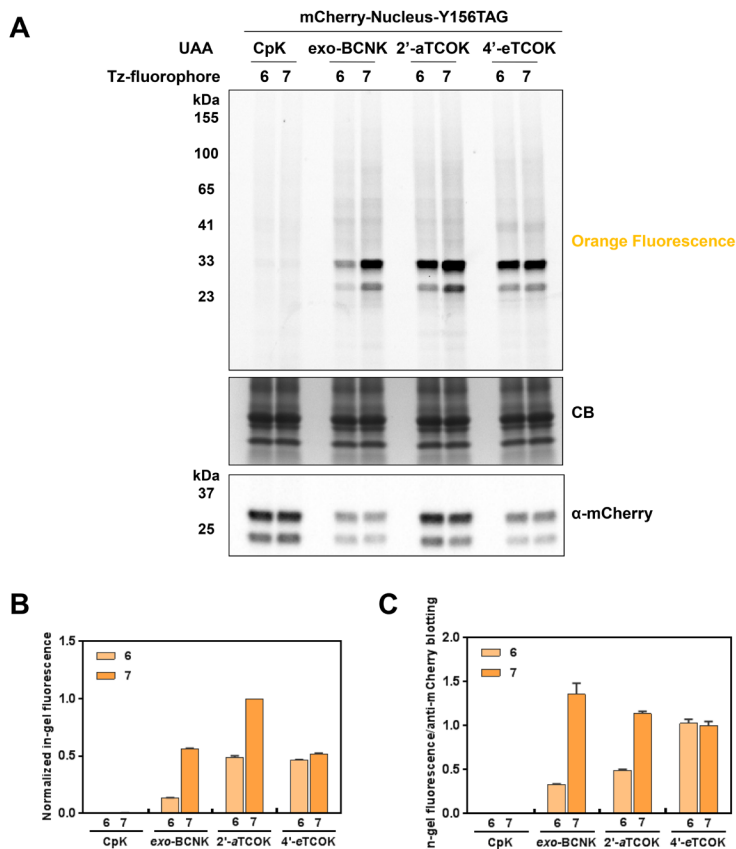


Figure S10. Bioorthogonal fluorescence labeling of mCherry-Nucleus-Y156TAG with orange tetrazine-fluorophores. Cells were co-transfected with pmCherry-Nucleus-Y156TAG and Mm-PyIRS-WT (wild-type PyIRS for CpK), Mm-PyIRS-AF (double mutant for exo-BCNK and 2'-aTCOK), or Mb-TCOKRS (TCOKRS for 4'-eTCOK) plasmids in the presence of CpK (50 μ M), exo-BCNK (50 μ M), 2'-aTCOK (50 μ M), or 4'-eTCOK (1 mM) for 16 h and further cultured in complete cell growth medium without UAA for another 6 h. Cells were then labeled with orange tetrazine-fluorophores **6-7** for 0.5 h, washed for 2 h, and then lysed for in-gel fluorescence, Coomassie Blue staining, and Western blotting analysis. (A) Representative gels for in-gel fluorescence, Coomassie Blue staining, and Western blotting analysis. (B) Bar graph showing the fluorescence labeling efficiency of mCherry-Nucleus-Y156TAG with tetrazine-fluorophores. Fluorescence intensity of every mCherry-Nucleus band was quantified and normalized to the most intense band of the corresponding gel, the intensity of which is set to 1. Data from three independent replicates were quantified and averaged for plotting the graphs. Data are mean \pm S.E.M., $n = 3$. (C) Bar graph showing the fluorescence labeling efficiency of mCherry-Nucleus with tetrazine-fluorophores relative to the protein expression levels. Intensities of in-gel fluorescence and anti-mCherry western blotting of every mCherry-Nucleus band were quantified, and then the fluorescence intensity was divided by the anti-mCherry western blotting intensity for each mCherry-Nucleus band. Data from three independent replicates were quantified and averaged for plotting the graphs. Data are mean \pm S.E.M., $n = 3$.

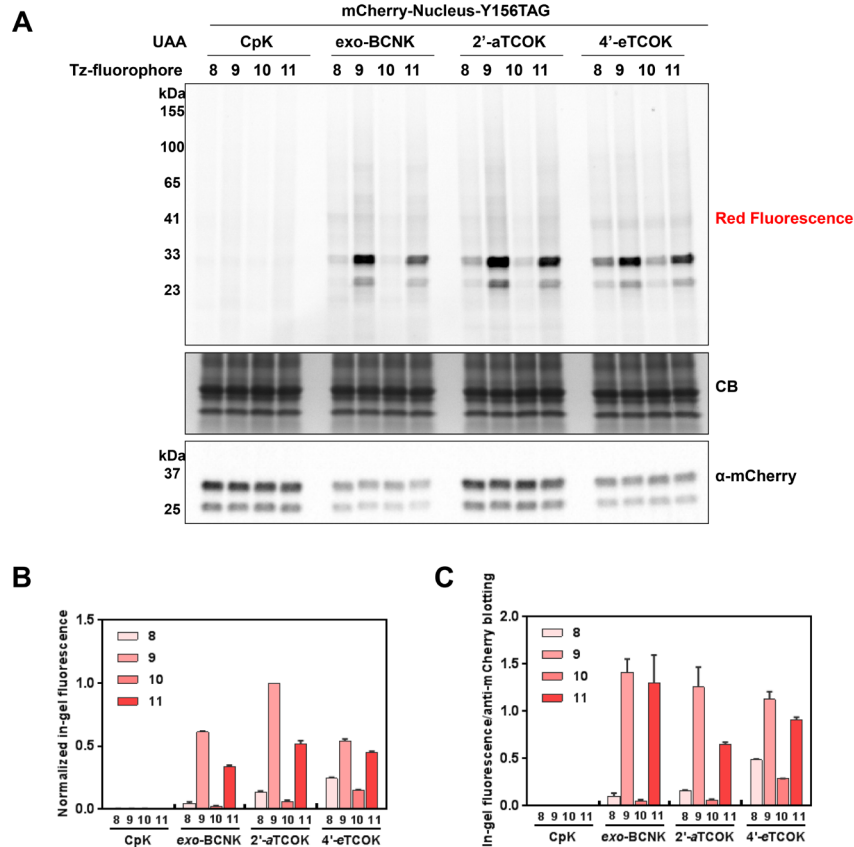


Figure S11. Bioorthogonal fluorescence labeling of mCherry-Nucleus-Y156TAG with red tetrazine-fluorophores. Cells were co-transfected with pmCherry-Nucleus-Y156TAG and Mm-PyIRS-WT (wild-type PyIRS for CpK), Mm-PyIRS-AF (double mutant for exo-BCNK and 2'-aTCOK), or Mb-TCOKRS (TCOKRS for 4'-eTCOK) plasmids in the presence of CpK (50 μ M), exo-BCNK (50 μ M), 2'-aTCOK (50 μ M), or 4'-eTCOK (1 mM) for 16 h and further cultured in complete cell growth medium without UAA for another 6 h. Cells were then labeled with red tetrazine-fluorophores **8-11** for 0.5 h, washed for 2 h, and then lysed for in-gel fluorescence, Coomassie Blue staining, and Western blotting analysis. (A) Representative gels for in-gel fluorescence, Coomassie Blue staining, and Western blotting analysis. (B) Bar graph showing the fluorescence labeling efficiency of mCherry-Nucleus-Y156TAG with tetrazine-fluorophores. Fluorescence intensity of every mCherry-Nucleus band was quantified and normalized to the most intense band of the corresponding gel, the intensity of which is set to 1. Data from three independent replicates were quantified and averaged for plotting the graphs. Data are mean \pm S.E.M., $n = 3$. (C) Bar graph showing the fluorescence labeling efficiency of mCherry-Nucleus with tetrazine-fluorophores relative to the protein expression levels. Intensities of in-gel fluorescence and anti-mCherry western blotting of every mCherry-Nucleus band were quantified, and then the fluorescence intensity was divided by the anti-mCherry western blotting intensity for each mCherry-Nucleus band. Data from three independent replicates were quantified and averaged for plotting the graphs. Data are mean \pm S.E.M., $n = 3$.

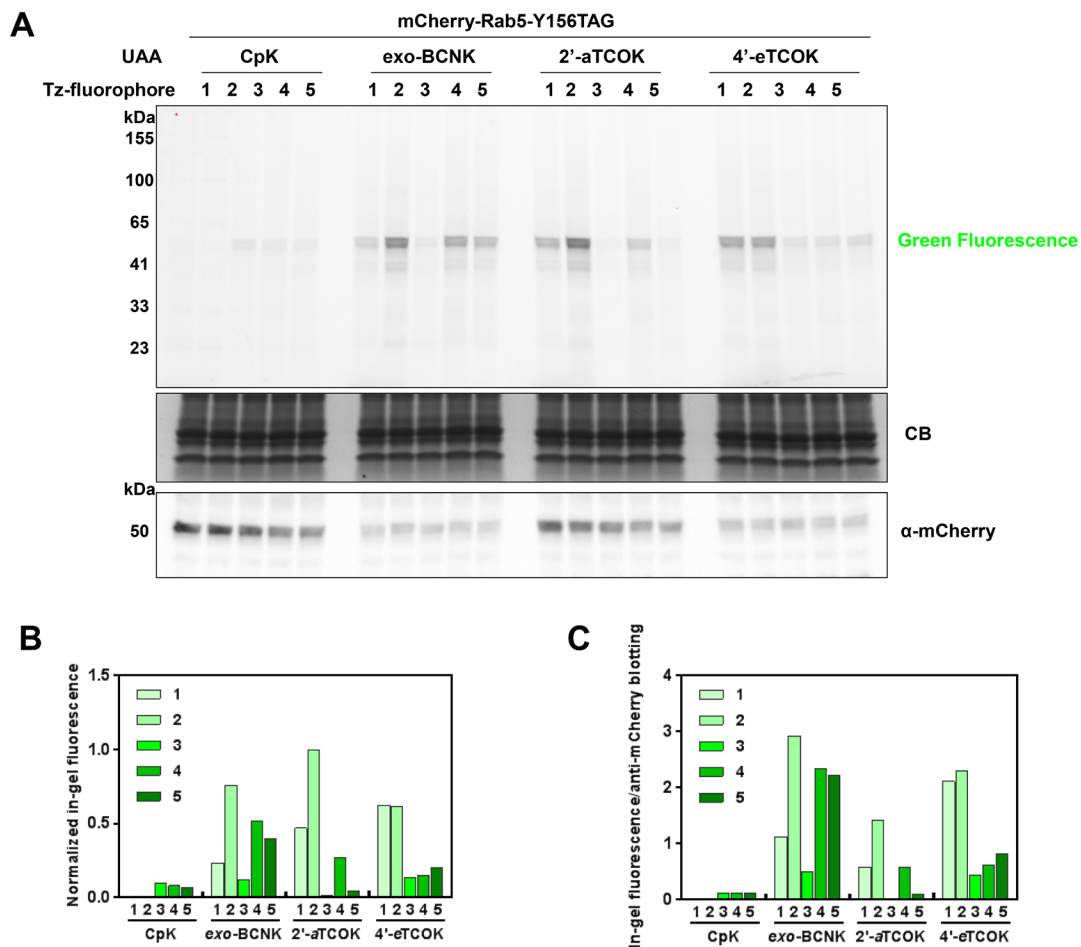


Figure S12. Bioorthogonal fluorescence labeling of mCherry-Rab5-Y156TAG with green tetrazine-fluorophores. Cells were co-transfected with pmCherry-Rab5-Y156TAG and Mm-PyIRS-WT (wild-type PyIRS for CpK), Mm-PyIRS-AF (double mutant for exo-BCNK and 2'-aTCOK), or Mb-TCOKRS (TCOKRS for 4'-eTCOK) plasmids in the presence of CpK (50 μ M), exo-BCNK (50 μ M), 2'-aTCOK (50 μ M), or 4'-eTCOK (1 mM) for 16 h and further cultured in complete cell growth medium without UAA for another 6 h. Cells were then labeled with green tetrazine-fluorophores **1-5** for 0.5 h, washed for 2 h, and then lysed for in-gel fluorescence, Coomassie Blue staining, and Western blotting analysis. (A) Representative gels for in-gel fluorescence, Coomassie Blue staining, and Western blotting analysis. (B) Bar graph showing the fluorescence labeling efficiency of mCherry-Rab5-Y156TAG with tetrazine-fluorophores. Fluorescence intensity of every mCherry-Rab5 band was quantified and normalized to the most intense band of the corresponding gel, the intensity of which is set to 1. (C) Bar graph showing the fluorescence labeling efficiency of mCherry-Rab5 with tetrazine-fluorophores relative to the protein expression levels. Intensities of in-gel fluorescence and anti-mCherry western blotting of every mCherry-Rab5 band were quantified, and then the fluorescence intensity was divided by the anti-mCherry western blotting intensity for each mCherry-Rab5 band.

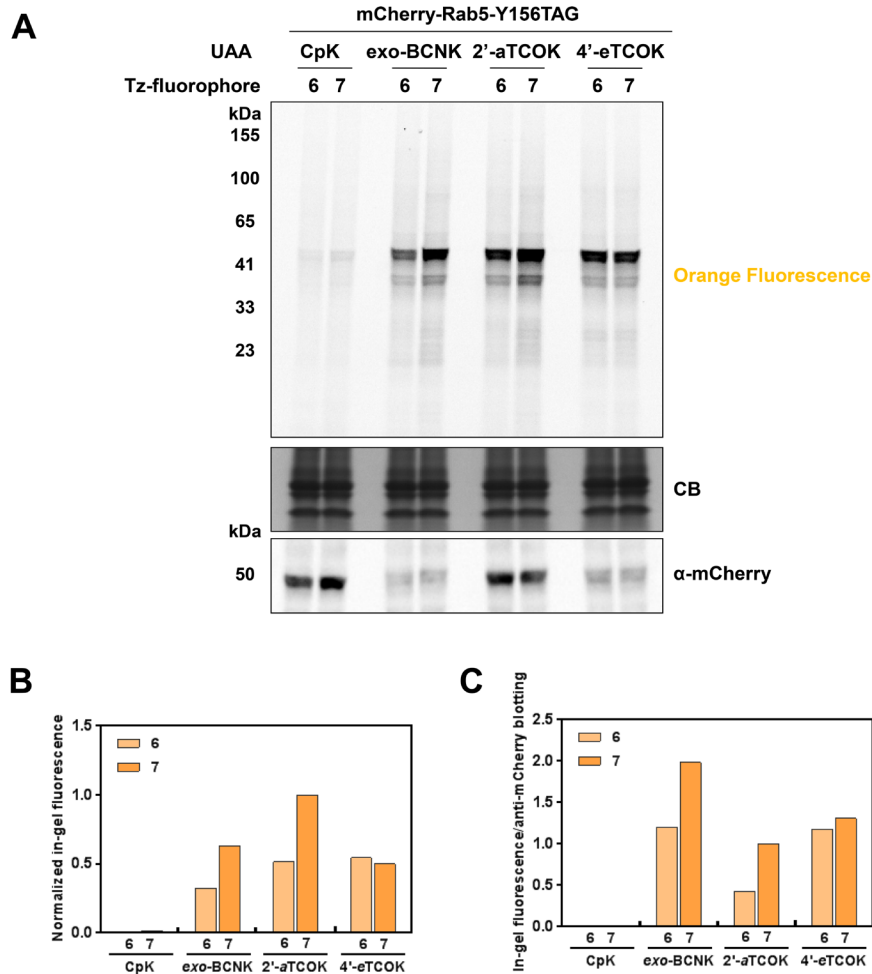


Figure S13. Bioorthogonal fluorescence labeling of mCherry-Rab5-Y156TAG with orange tetrazine-fluorophores. Cells were co-transfected with pmCherry-Rab5-Y156TAG and Mm-PyIRS-WT (wild-type PyIRS for CpK), Mm-PyIRS-AF (double mutant for exo-BCNK and 2'-aTCOK), or Mb-TCOKRS (TCOKRS for 4'-eTCOK) plasmids in the presence of CpK (50 μ M), exo-BCNK (50 μ M), 2'-aTCOK (50 μ M), or 4'-eTCOK (1 mM) for 16 h and further cultured in complete cell growth medium without UAA for another 6 h. Cells were then labeled with orange tetrazine-fluorophores **6-7** for 0.5 h, washed for 2 h, and then lysed for in-gel fluorescence, Coomassie Blue staining, and Western blotting analysis. (A) Representative gels for in-gel fluorescence, Coomassie Blue staining, and Western blotting analysis. (B) Bar graph showing the fluorescence labeling efficiency of mCherry-Rab5-Y156TAG with tetrazine-fluorophores. Fluorescence intensity of every mCherry-Rab5 band was quantified and normalized to the most intense band of the corresponding gel, the intensity of which is set to 1. (C) Bar graph showing the fluorescence labeling efficiency of mCherry-Rab5 with tetrazine-fluorophores relative to the protein expression levels. Intensities of in-gel fluorescence and anti-mCherry western blotting of every mCherry-Rab5 band were quantified, and then the fluorescence intensity was divided by the anti-mCherry western blotting intensity for each mCherry-Rab5 band.

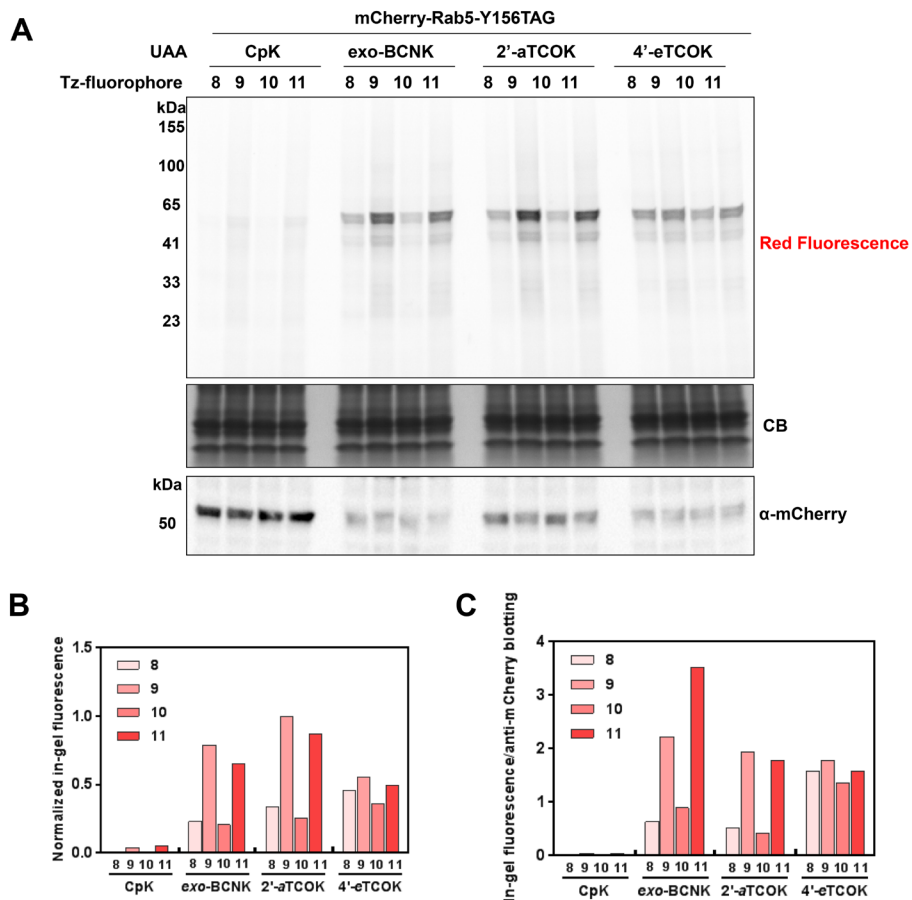


Figure S14. Bioorthogonal fluorescence labeling of mCherry-Rab5-Y156TAG with red tetrazine-fluorophores. Cells were co-transfected with pmCherry-Rab5-Y156TAG and Mm-PylRS-WT (wild-type PylRS for CpK), Mm-PylRS-AF (double mutant for exo-BCNK and 2'-aTCOK), or Mb-TCOKRS (TCOKRS for 4'-eTCOK) plasmids in the presence of CpK (50 μ M), exo-BCNK (50 μ M), 2'-aTCOK (50 μ M), or 4'-eTCOK (1 mM) for 16 h and further cultured in complete cell growth medium without UAA for another 6 h. Cells were then labeled with red tetrazine-fluorophores **8-11** for 0.5 h, washed for 2 h, and then lysed for in-gel fluorescence, Coomassie Blue staining, and Western blotting analysis. (A) Representative gels for in-gel fluorescence, Coomassie Blue staining, and Western blotting analysis. (B) Bar graph showing the fluorescence labeling efficiency of mCherry-Rab5-Y156TAG with tetrazine-fluorophores. Fluorescence intensity of every mCherry-Rab5 band was quantified and normalized to the most intense band of the corresponding gel, the intensity of which is set to 1. (C) Bar graph showing the fluorescence labeling efficiency of mCherry-Rab5 with tetrazine-fluorophores relative to the protein expression levels. Intensities of in-gel fluorescence and anti-mCherry western blotting of every mCherry-Rab5 band were quantified, and then the fluorescence intensity was divided by the anti-mCherry western blotting intensity for each mCherry-Rab5 band.

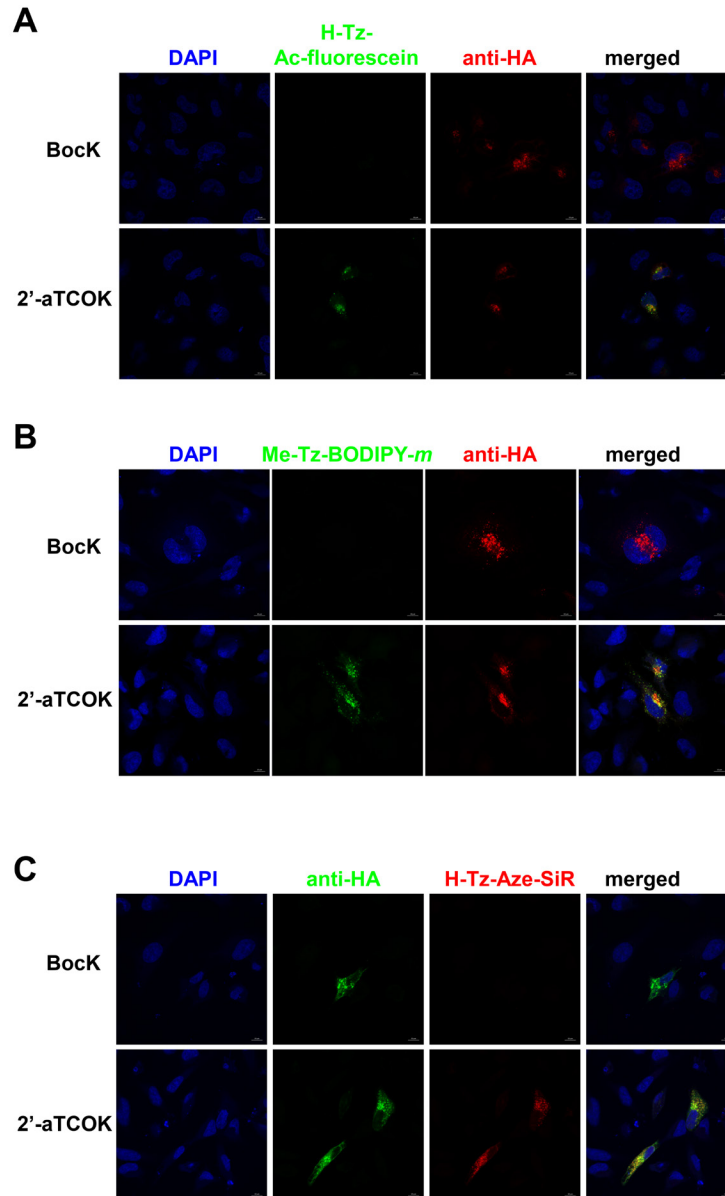


Figure S15. Specific fluorescence labeling and imaging of HA-IFITM3-F8TAG with H-Tz-Ac-fluorescein, Me-Tz-BODIPY-*m*, or H-Tz-Aze-SiR in the presence of different UAAs. HeLa cells were co-transfected with pCMV-HA-IFITM3-F8TAG and pEF1 α -FLAG-Mm-PylRS wild-type or AF double mutant plasmids in the presence of UAAs (50 μ M) for 16 h and further cultured in complete cell growth medium without UAA for another 6 h. Cells were then labeled with H-Tz-Ac-fluorescein, Me-Tz-BODIPY-*m*, or H-Tz-Aze-SiR (500 nM) for 0.5 h and washed for 2 h before fixation with 4% formaldehyde. After permeabilization with Triton X-100, cells were immunostained with anti-HA-Alexa Fluor 594 or anti-HA-Alexa Fluor 488 conjugate and imaged by confocal fluorescence microscopy. DAPI (blue) is used to stain nuclei. For incorporating CpK, Mm-PylRS wild-type was used, while the AF double mutant was used for incorporating 2'-aTCOK. Scale bars = 10 μ m.

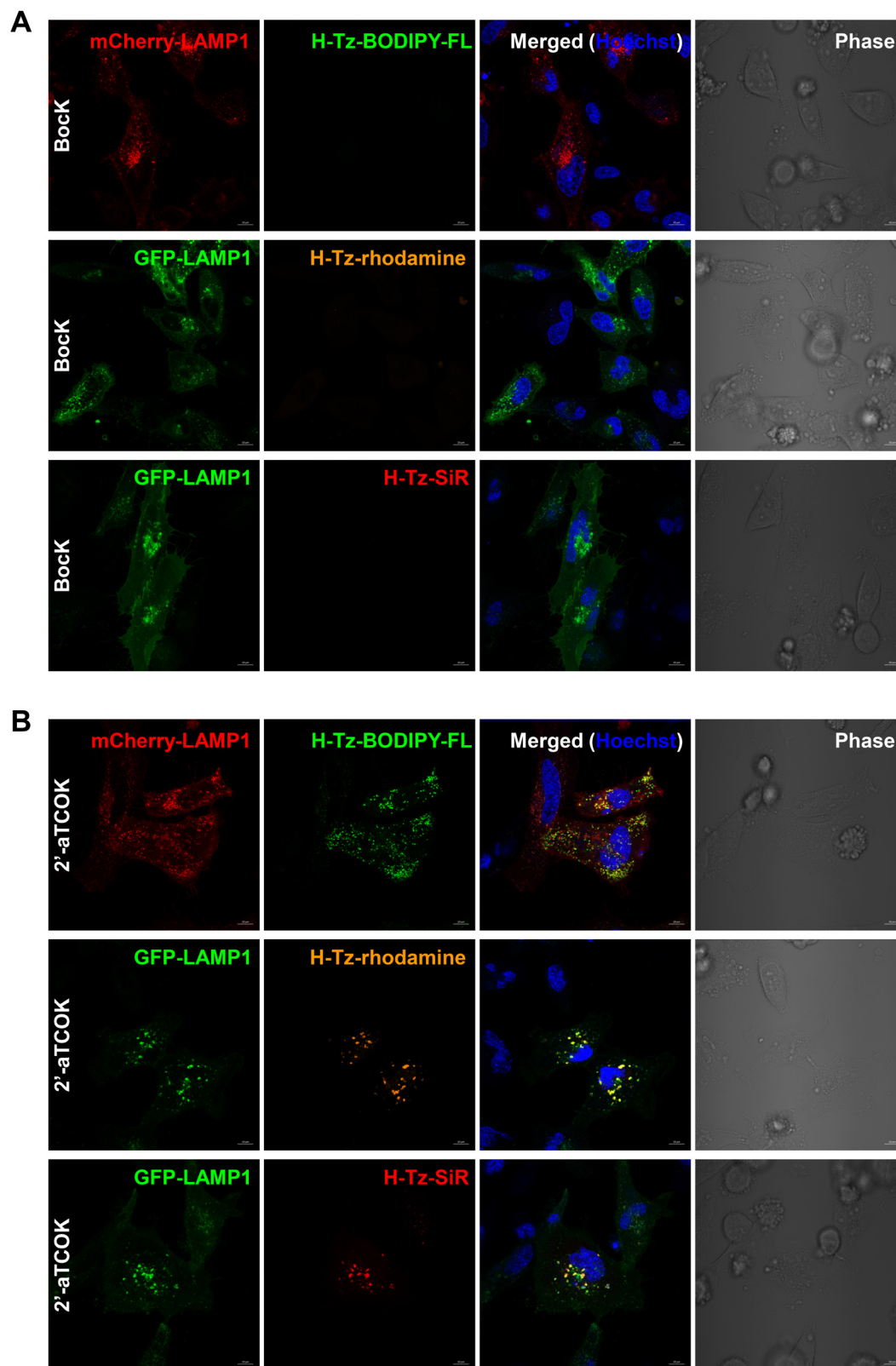


Figure S16. Complete Figure 5. Live cell bioorthogonal fluorescence imaging of HA-IFITM3-F8UAA with tetrazine-fluorophores.

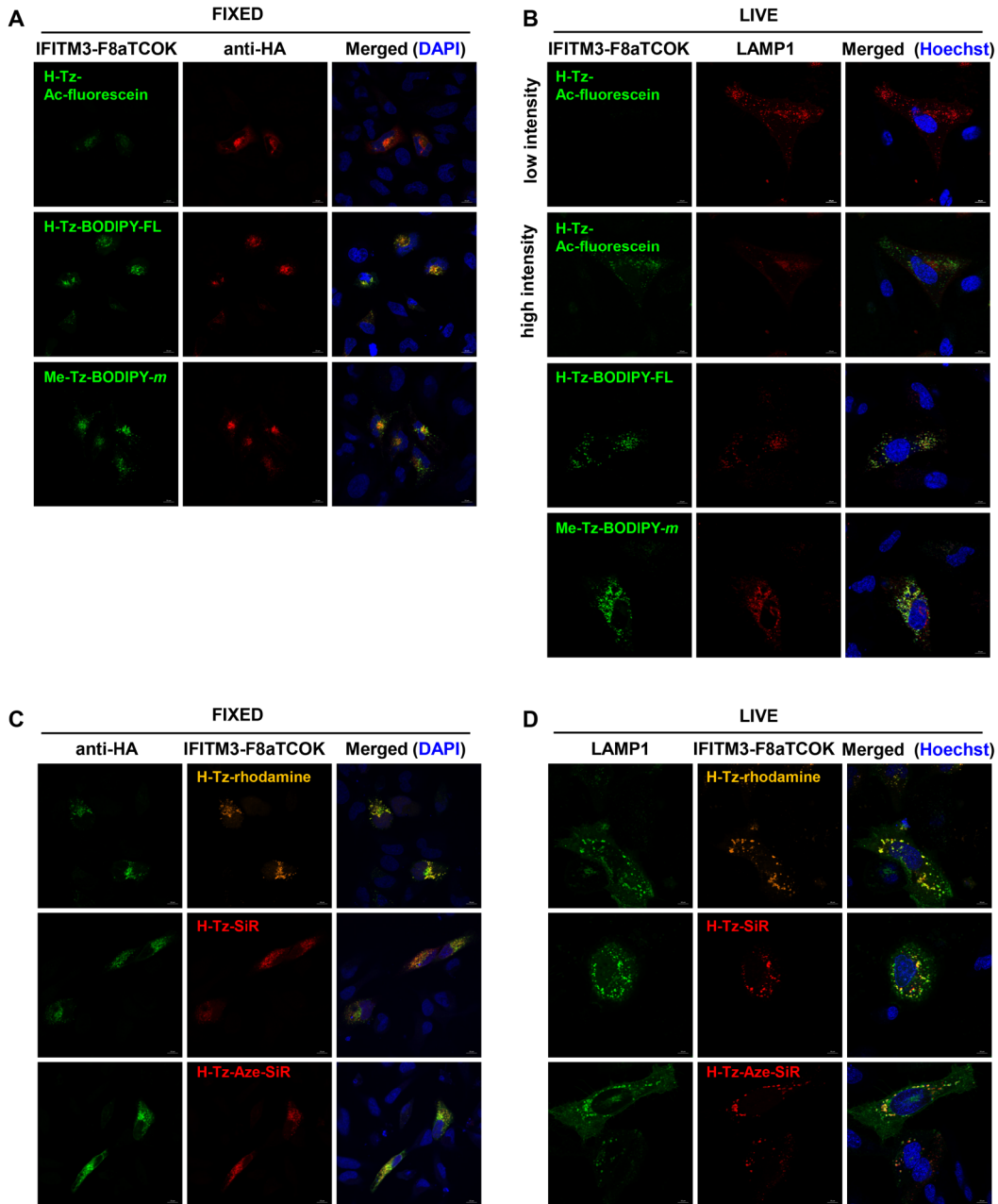


Figure S17. Comparison of fixed cell imaging and live cell imaging of IFITM3-F8aTCOK with distinct tetrazine-fluorophores. Fixed cell samples were prepared as described above, whereas live cell samples were prepared as described in caption of Figure 4. IFITM3-F8aTAG was expressed in HeLa cells in the presence of 2'-aTCOK (50 μ M). Identical confocal microscope settings were used for samples labeled with H-Tz-Ac-fluorescein (low laser intensity panel), H-Tz-BODIPY-FL, and Me-Tz-BODIPY-*m*. Imaging with H-Tz-Ac-fluorescein requires higher laser intensity and shows higher fluorescence background inside the live cells than imaging with H-Tz-BODIPY-FL and Me-Tz-BODIPY-*m*. Identical confocal microscope settings were used for samples labeled with H-Tz-SiR and H-Tz-Aze-SiR. Scale bars = 10 μ m.

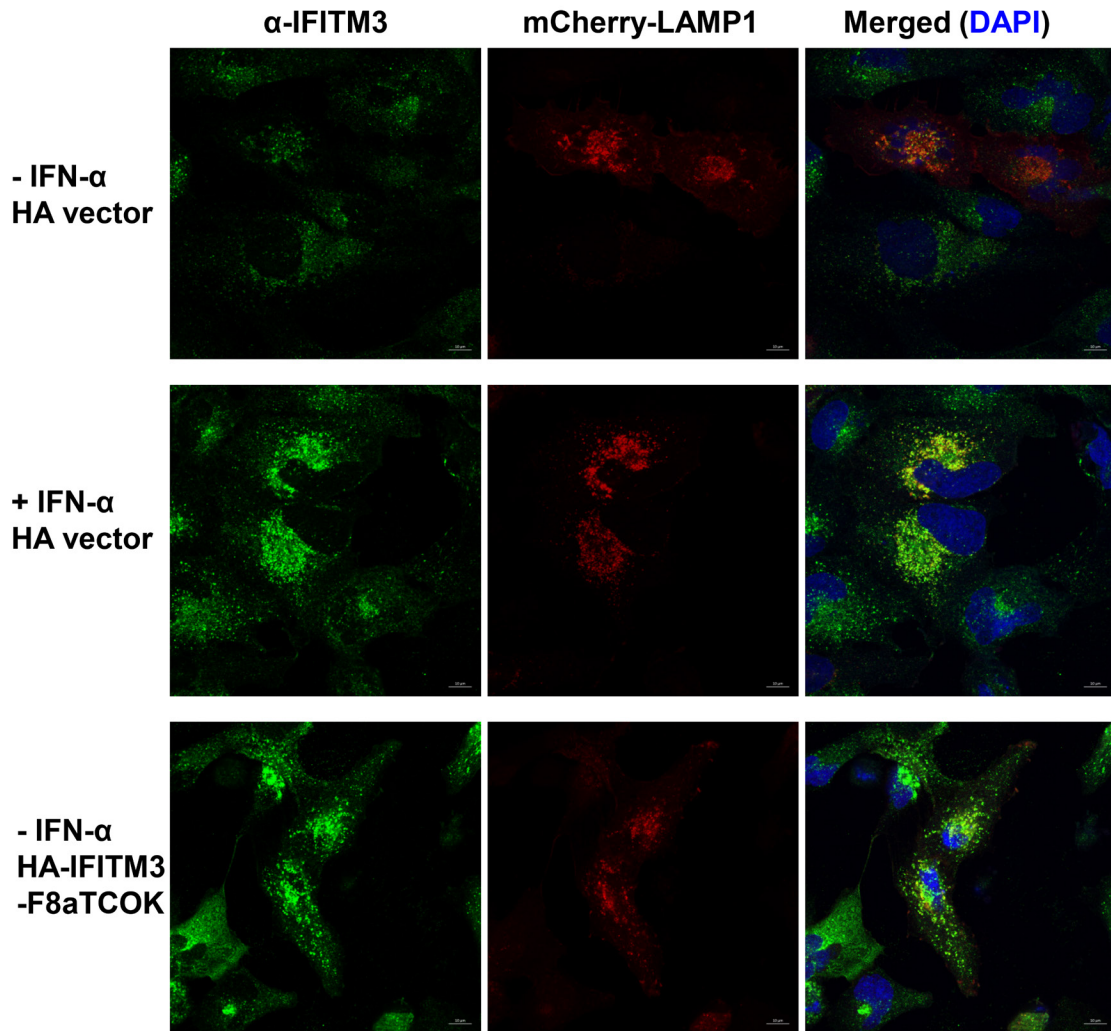


Figure S18. Immunofluorescence imaging of endogenous and overexpressed IFITM3. HeLa cells were transfected with pCMV-HA vector or pCMV-HA-IFITM3-F8TAG, pEF1 α -FLAG-Mm-PyIRS-AF mutant, and mCherry-LAMP1 plasmids in the presence of 2'-aTCOK (50 μ M) for 16 h and further treated with or without IFN- α for 8 h. Cells were then fixed with formaldehyde, permeabilized with Triton X-100, and immunostained with rabbit anti-IFITM3 and anti-rabbit-Alexa Fluor 488 conjugate for confocal fluorescence imaging. DAPI (blue) is used to stain nuclei. Images were taken under identical confocal microscope settings. Scale bars = 10 μ m.

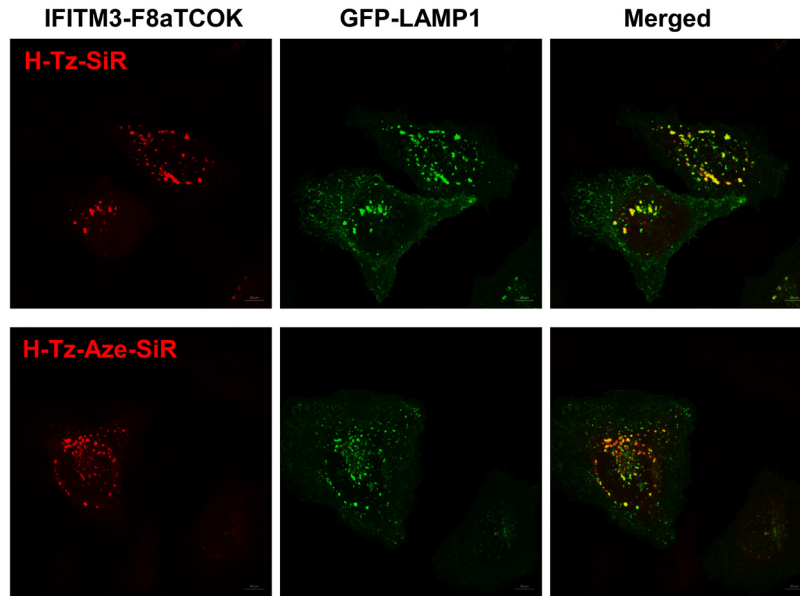


Figure S19. No-wash imaging of IFITM3-F8TAG with H-Tz-SiR/Aze-SiR in live cells. HeLa cells were co-transfected with pCMV-HA-IFITM3-F8TAG, pEF1 α -FLAG-Mm-PyIRS-AF mutant, and GFP-LAMP1 plasmids in the presence of 2'-aTCOK (50 μ M) for 16 h and further cultured in complete cell growth medium without UAA for another 6 h. Cells were then labeled with H-Tz-SiR or H-Tz-Aze-SiR (500 nM) for 0.5 h and directly imaged with confocal fluorescence microscopy. Images were taken under identical confocal microscope settings. Scale bars = 10 μ m.

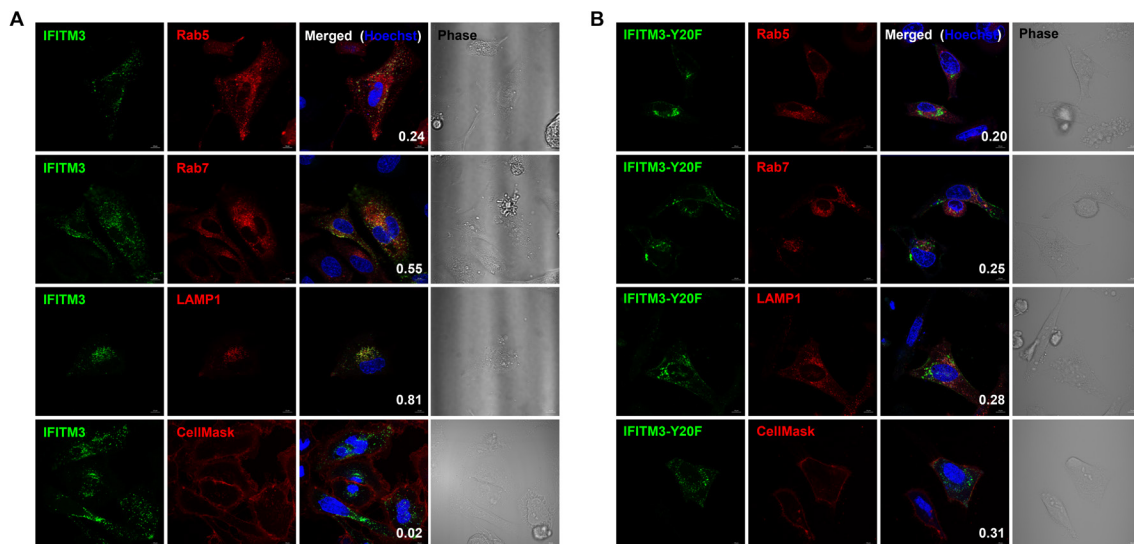


Figure S20. Complete Figure 6. Live cell bioorthogonal fluorescence imaging of HA-IFITM3-F8UAA localization with H-Tz-BODIPY-FL.

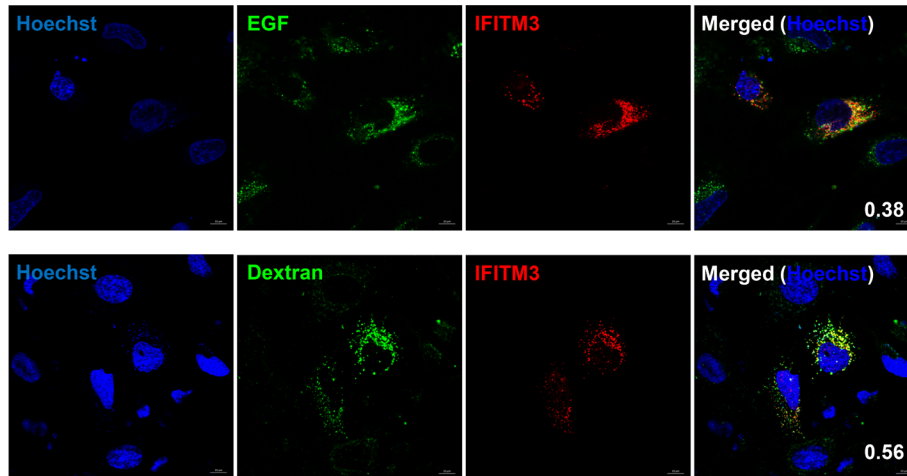


Figure S21. Co-localization of IFITM3 with exogenous endocytosis cargoes. HeLa cells were co-transfected with pCMV-HA-IFITM3-F8TAG and pEF1 α -FLAG-Mm-PyIRS-AF mutant plasmids in the presence of 2'-aTCOK (50 μ M) for 16 h and further cultured in complete cell growth medium without UAA for another 6 h. Cells were then labeled with H-Tz-SiR (500 nM) for 0.5 h, washed for 2 h, and treated with pHrodo Green-Dextran or pHrodo Green-EGF for 30 min before imaged with confocal fluorescence microscopy. Hoechst (blue) is used to stain nuclei. Scale bars = 10 μ m.

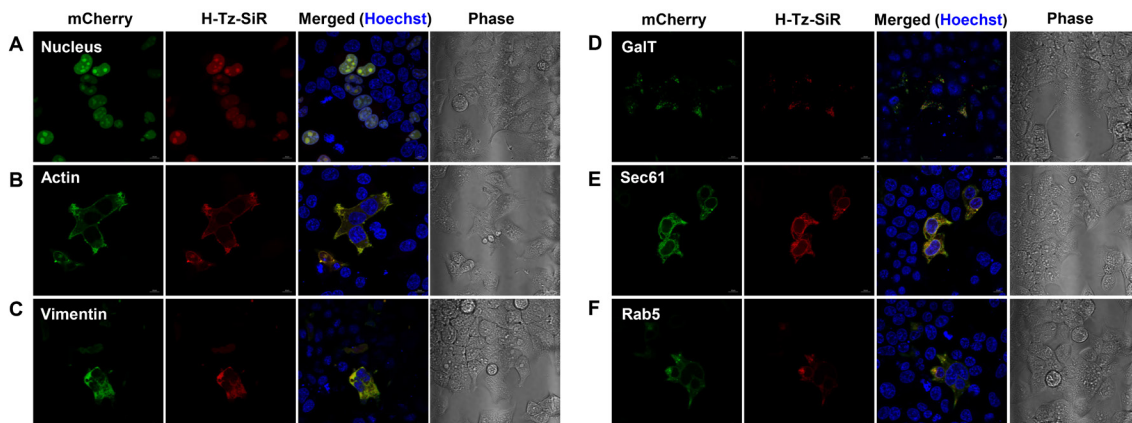


Figure S22. Complete Figure 8. Live cell bioorthogonal fluorescence imaging of benchmark intracellular proteins.

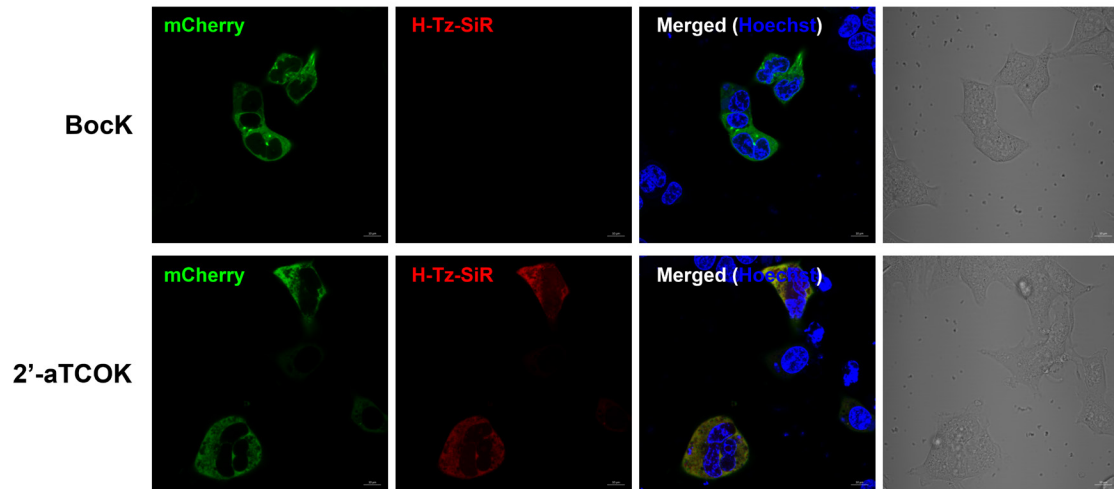
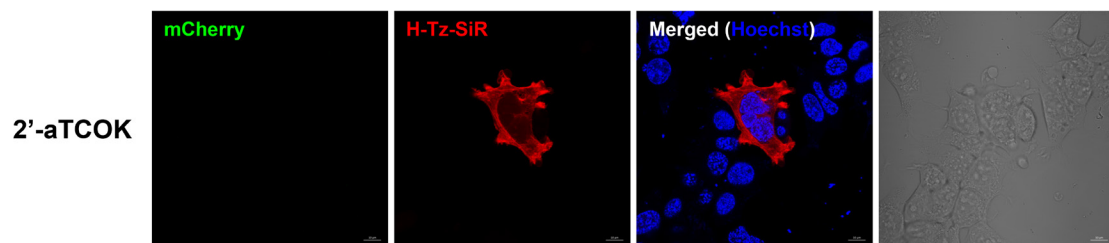
A**B**

Figure S23. Live cell imaging of mCherry-Vimentin-N116TAG and HA-Actin-K118TAG. (A) HEK293T cells expressing mCherry-Vimentin-N116TAG in the presence of Bock or 2'-aTCOK were labeled with H-Tz-SiR (red) and stained with Hoechst (blue) for live cell imaging. (B) HEK293T cells expressing HA-Actin-K118TAG in the presence of 2'-aTCOK were labeled with H-Tz-SiR (red) and stained with Hoechst (blue) for live cell imaging with confocal microscopy. Scale bars = 10 μ m.

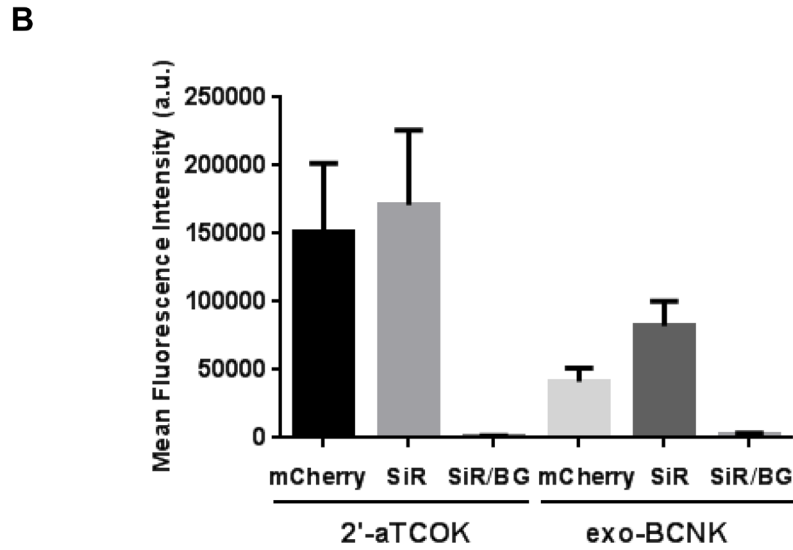
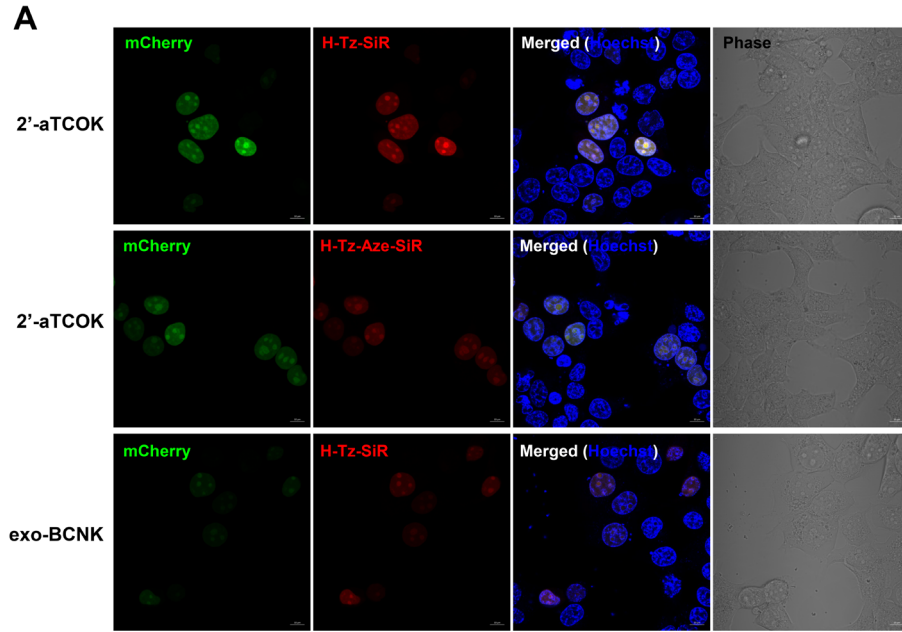


Figure S24. Comparison of 2'-aTCOK and exo-BCNK for live cell imaging of mCherry-Nucleus-Y156TAG. (A) HEK293T cells expressing mCherry-Nucleus-Y156TAG in the presence of 2'-aTCOK or exo-BCNK were labeled with H-Tz-SiR (red) or H-Tz-Aze-SiR (red) and stained with Hoechst (blue) for live cell imaging with confocal microscopy. Scale bars = 10 μ m. (B) Quantification of fluorescence imaging in (A). mCherry and SiR represents mean fluorescence intensity of cells in mCherry and SiR channel, respectively, while SiR/BG is mean background fluorescence intensity of untransfected cells in SiR channel. Data are shown in mean \pm S.E.M., n = 20 – 40 cells. The signal-to-noise ratios of 2'-aTCOK and exo-BCNK labeling are estimated to be \sim 100 and 30, respectively.

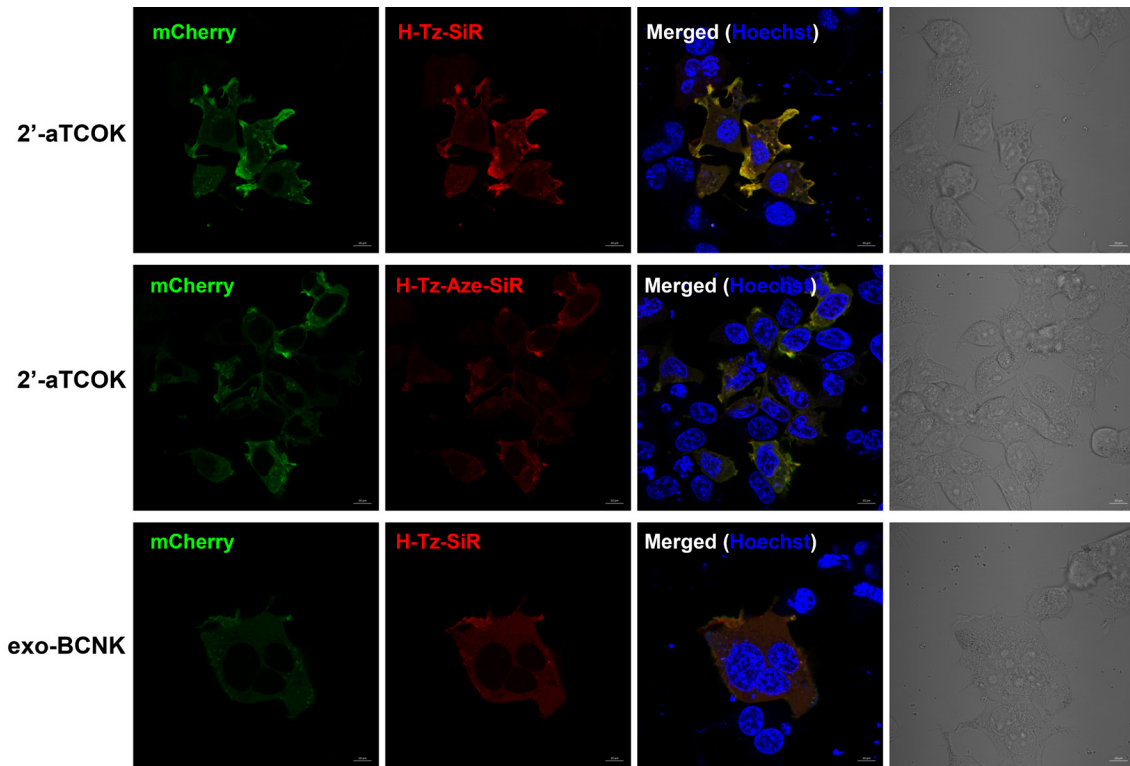


Figure S25. Live cell imaging of mCherry-Actin-Y156TAG. HEK293T cells expressing mCherry-Actin-Y156TAG in the presence of 2'-aTCOK or exo-BCNK were labeled with H-Tz-SiR or H-Tz-Aze-SiR (red) and stained with Hoechst (blue) for live cell imaging with confocal microscopy. Scale bars = 10 μ m.

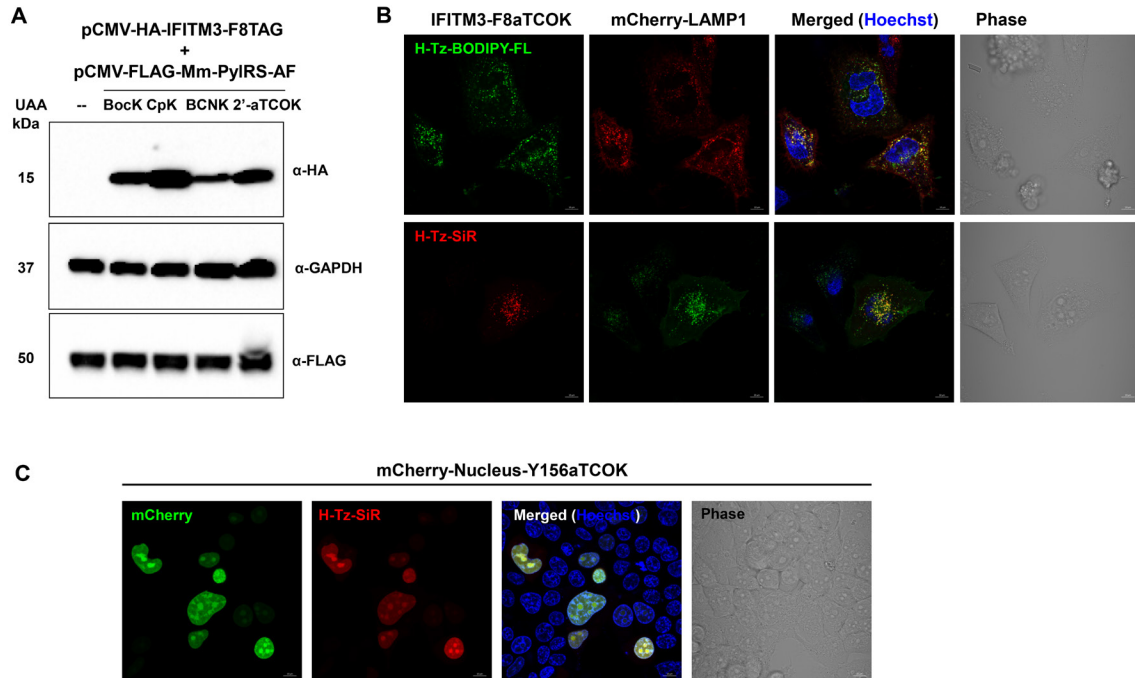


Figure S26. Expression and imaging of IFITM3-F8TAG by using pCMV-FLAG-Mm-PyIRS-AF plasmid (Figure S1C) in live cells. (A) Western blotting analysis of IFITM3-F8TAG expression in the presence of UAA (50 μ M) by using pCMV-FLAG-Mm-PyIRS-AF mutant plasmid. (B) Imaging of IFITM3-F8aTCOK in HeLa cells transfected with pCMV-FLAG-Mm-PyIRS-AF and labeled with H-Tz-BDP-FL or H-Tz-SiR (250 nM, 0.5 h). (C) Imaging of mCherry-Nucleus-Y156aTCOK in HeLa cells transfected with pCMV-FLAG-Mm-PyIRS-AF and labeled with H-Tz-SiR (250 nM, 0.5 h). Hoechst (blue) is used to stain nuclei. Scale bars = 10 μ m.

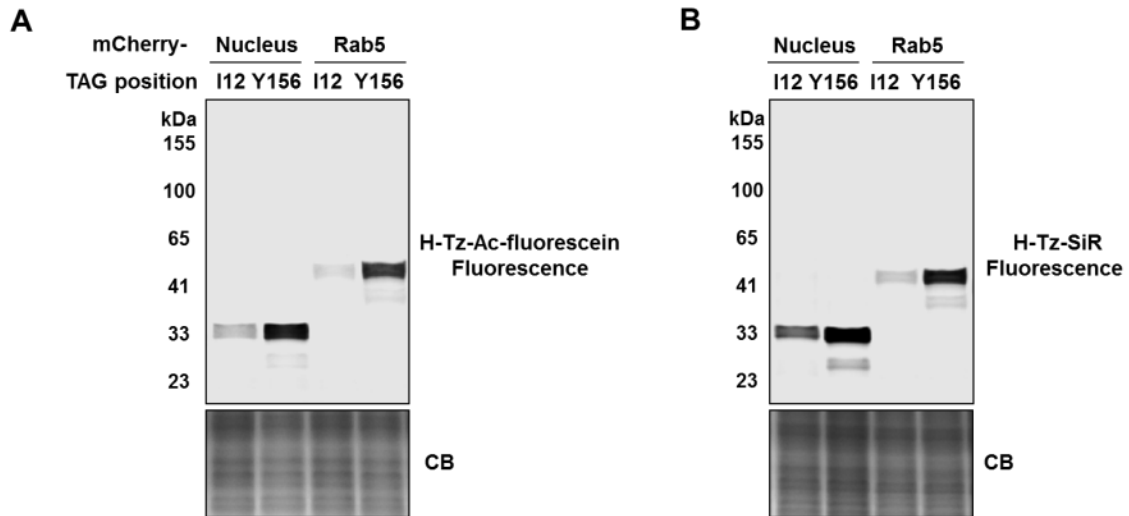


Figure S27. Comparison of fluorescence labeling efficiency at different amino acid positions of mCherry. HEK293T cells were co-transfected with pmCherry-Nucleus or pmCherry-Rab5 bearing different TAG codon positions (I12TAG or Y156TAG) and pEF1 α -FLAG-Mm-PylRS-AF mutant plasmids in the presence of 2'-aTCOK (50 μ M) for 16 h and further cultured in complete cell growth medium without UAA for another 6 h. Cells were then labeled with (A) H-Tz-Ac-fluorescein or (B) H-Tz-SiR (500 nM) for 0.5 h, washed for 2 h, and then lysed for in-gel fluorescence and Coomassie Blue staining (CB). As shown here, 2'-aTCOK at Y156 position is more efficiently labeled by both H-Tz-Ac-fluorescein and H-Tz-SiR than at I12 position.

Supplemental Video S1: Time-lapse imaging of IFITM3 trafficking with exogenous dextran particles in live cells. IFITM3 was labeled with green fluorophore H-Tz-BODIPY-FL, while dextran was labeled with a red fluorophore.

Synthetic methods and materials

Unless otherwise noted, chemicals were obtained from either Sigma-Aldrich or Acros and were used as received. Reactions were performed in oven-dried flasks under Ar protection and monitored by analytical TLC on Merck silica gel plates with fluorescent indicator on glass (5–20 μm , 60 \AA). Compounds on TLC were visualized by UV light (254 nm) and staining with ceric ammonium molybdate (CAM) or basic KMnO_4 . Fisher S704 silica gel (60-200 Mesh, chromatographic grade) was used for flash column chromatography. ^1H and ^{13}C NMR spectra were obtained on a Bruker Avance DMX600 spectrometer in CDCl_3 using tetramethylsilane (TMS) as an internal standard or in d^6 -DMSO. Chemical shifts are reported in δ ppm, and J values are reported in Hz. MALDI-TOF mass spectra were obtained on an Applied Biosystems Voyager-DE. Analytical and preparative HPLC was conducted on a Waters 1525 Binary HPLC Pump system equipped with a XBridge C18 analytical or preparative column (5 μm , 4.6 x 150 mm or 19 x 150 mm) and a UV-Vis wavelength detector. Compounds were eluted with the acetonitrile/water/TFA solvent system.

Unnatural amino acids

BocK (N ϵ -Boc-L-lysine) was purchased from Aldrich (359661-5G). CpK, 2'-aTCOK, exo-BCNK, endo-BCNK, 4'-aTCOK, and 4'-eTCOK were synthesized in the laboratory according to previous reports.^{5,6} Their characterization data including ^1H and ^{13}C NMR are in accordance with those in literature.^{5,6} The NMR data and spectra are shown below. UAA powders were dissolved at 100 mM concentrations in 0.2 M NaOH with 20% DMSO to be the stock solutions, which were stored at $-20\text{ }^\circ\text{C}$.

Characterizations of UAAs:

endo-BCNK

^1H NMR (600 MHz, MeOD/ D_2O) δ 4.14 (d, J = 7.9 Hz, 2H), 3.65 (t, J = 5.6 Hz, 1H), 3.12 (s, 2H), 2.42 – 2.10 (m, 4H), 1.92 – 1.77 (m, 4H), 1.60 – 1.35 (m, 7H), 1.07 – 0.95 (m, 2H). ^{13}C NMR (151 MHz, MeOD/ D_2O) δ 174.09, 158.57, 99.62, 63.11, 54.81, 54.78, 40.03, 30.36, 28.93, 28.67, 21.92, 20.67, 19.86, 17.41.

exo-BCNK

^1H NMR (600 MHz, MeOD/ D_2O) δ 3.94 (d, J = 6.8 Hz, 2H), 3.61 (t, J = 5.8 Hz, 1H), 3.11 (t, J = 6.5 Hz, 2H), 2.38 (d, J = 13.1 Hz, 2H), 2.25 (t, J = 13.7 Hz, 2H), 2.12 (d, J = 15.6 Hz, 2H), 1.94 – 1.77 (m, 2H), 1.58 – 1.49 (m, 2H), 1.47 – 1.33 (m, 4H), 0.74 – 0.66 (m, 3H). ^{13}C NMR (151 MHz, MeOD/ D_2O) δ 173.89, 158.42, 99.05, 69.07, 54.76, 39.98, 32.90, 30.46, 29.04, 23.50, 22.67, 21.98, 20.57.

2'-aTCOK

^1H NMR (600 MHz, MeOD) δ 5.90 – 5.76 (m, 1H), 5.55 (d, J = 16.3 Hz, 1H), 5.23 (s, 1H), 3.53 (s, 1H), 3.12 (s, 2H), 2.45 (d, J = 10.3 Hz, 1H), 2.10 – 1.94 (m, 3H), 1.94 – 1.77 (m, 3H), 1.72 (t, J = 13.6 Hz, 1H), 1.67 – 1.59 (m, 1H), 1.58 – 1.38 (m, 5H), 1.16 (t, J = 10.6

Hz, 1H), 0.94 – 0.81 (m, 1H). ^{13}C NMR (151 MHz, MeOD) δ 173.02, 157.11, 131.56, 131.17, 73.65, 54.72, 40.25, 39.87, 35.64, 35.36, 30.56, 29.22, 28.68, 23.80, 22.15, 22.10.

4'-aTCOK

^1H NMR (600 MHz, DMSO) δ 5.61 (dd, $J = 19.7, 7.2$ Hz, 1H), 5.51 – 5.42 (m, 1H), 4.67 (dd, $J = 9.6, 4.8$ Hz, 1H), 3.68 (s, 1H), 3.04 – 2.92 (m, 2H), 2.26 – 1.94 (m, 5H), 1.86 – 1.54 (m, 5H), 1.51 – 1.22 (m, 5H), 1.20 – 1.09 (m, 1H). ^{13}C NMR (151 MHz, DMSO) δ 171.28, 156.41, 135.53, 131.96, 68.87, 52.59, 40.85, 34.35, 32.55, 30.07, 30.02, 29.40, 27.85, 22.16.

4'-eTCOK

^1H NMR (600 MHz, $\text{D}_2\text{O}/\text{DMSO}$) δ 5.73 – 5.60 (m, 1H), 5.60 – 5.48 (m, 1H), 4.25 (s, 1H), 3.69 (s, 1H), 3.08 (s, 2H), 2.33 (s, 3H), 1.95 – 1.82 (m, 6H), 1.62 (s, 3H), 1.54 – 1.44 (m, 2H), 1.38 – 1.35 (m, 2H). ^{13}C NMR (151 MHz, $\text{D}_2\text{O}/\text{DMSO}$) δ 174.50, 158.30, 135.59, 133.31, 81.66, 54.56, 40.43, 39.87, 33.73, 32.09, 30.59, 30.06, 28.66, 21.63.

Tetrazine-fluorophores

5-Carboxyl-fluorescein diacetate (from Berry & Associates), BODIPY-FL acid (from AAT Bioquest), and 5-carboxyl-rhodamine (from Berry & Associates) were purchased from commercial sources. Me-BODIPY-*m*, 6-carboxyl-silicon-tetramethylrhodamine, and 6-carboxyl-silicon-azetidinerhodamine were synthesized in the laboratory according to previous reports.⁷⁻⁹ Tetrazine amines, including (4-(6-methyl-1,2,4,5-tetrazin-3-yl)phenyl)methanamine and (4-(1,2,4,5-tetrazin-3-yl)phenyl)methanamine, were synthesized in the laboratory as described before.¹⁰

Generally, tetrazine-fluorophore conjugates were synthesized by coupling the carboxyl acid derivatives of fluorophores with tetrazine amines. Briefly, to a solution of the carboxyl acid derivative of the fluorophore (1 equiv.) in anhydrous DMF were added DIPEA (5 equiv.), tetrazine amine (1.5 equiv.) and TBTU (1.2 equiv.) successively under Ar. The mixture was then stirred at room temperature under Ar overnight. After that, the mixture was concentrated and purified by silica gel flash column chromatography and reverse phase preparative HPLC. The purified compounds were characterized by NMR and MALDI-TOF-MS, which are consistent with literature reports.

MALDI-TOF-MS characterizations of known tetrazine-fluorophores:

Me-Tz-Ac-fluorescein **1**:¹¹ calcd. for $\text{C}_{35}\text{H}_{26}\text{N}_5\text{O}_8$ $[\text{M}+\text{H}]^+$ 644.18, found 644.3.
H-Tz-Ac-fluorescein **2**:¹¹ calcd. for $\text{C}_{34}\text{H}_{24}\text{N}_5\text{O}_8$ $[\text{M}+\text{H}]^+$ 630.16, found 630.4.
Me-Tz-BODIPY-FL **3**:¹² calcd. for $\text{C}_{24}\text{H}_{25}\text{BF}_2\text{N}_7\text{O}$ $[\text{M}+\text{H}]^+$ 476.22, found 476.2.
H-Tz-BODIPY-FL **4**:¹² calcd. for $\text{C}_{23}\text{H}_{23}\text{BF}_2\text{N}_7\text{O}$ $[\text{M}+\text{H}]^+$ 462.20, found 462.1.
Me-Tz-BODIPY-*m* **5**:⁷ calcd. for $\text{C}_{22}\text{H}_{22}\text{BF}_2\text{N}_6$ $[\text{M}+\text{H}]^+$ 419.20, found 419.3.

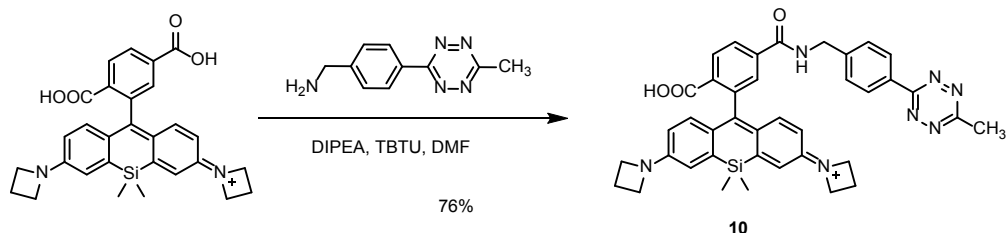
Me-Tz-rhodamine **6**:¹³ calcd. for C₃₅H₃₂N₇O₄ [M+H]⁺ 614.25, found 614.5.

H-Tz-rhodamine **7**:¹³ calcd. for C₃₄H₃₀N₇O₄ [M+H]⁺ 600.24, found 600.3.

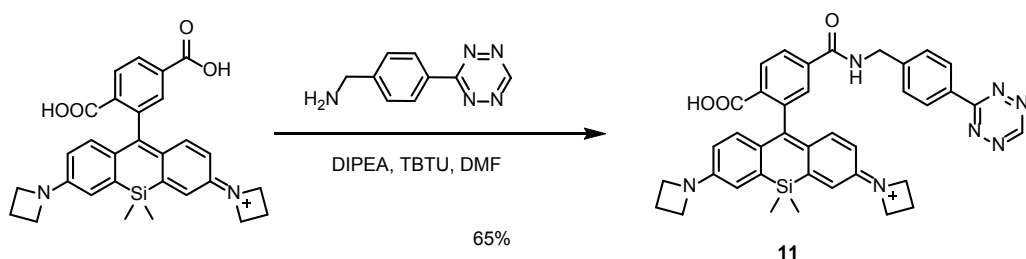
Me-Tz-SiR **8**:⁸ calcd. for C₃₇H₃₈N₇O₃Si [M+H]⁺ 656.28, found 656.3.

H-Tz-SiR **9**:¹⁴ calcd. for C₃₆H₃₆N₇O₃Si [M+H]⁺ 642.26, found 642.1.

Characterizations of new tetrazine-fluorophores:



Me-Tz-Aze-SiR **10** was synthesized as described above in 76% yield. ¹H NMR (600 MHz, CDCl₃) δ 8.56 (d, *J* = 8.2 Hz, 2H), 8.02 (dd, *J* = 8.0, 0.9 Hz, 1H), 7.96 (dd, *J* = 8.0, 0.9 Hz, 1H), 7.65 (s, 1H), 7.54 (d, *J* = 8.2 Hz, 2H), 6.74 (d, *J* = 8.7 Hz, 2H), 6.64 (d, *J* = 2.5 Hz, 2H), 6.52 (t, *J* = 5.6 Hz, 1H), 6.26 (dd, *J* = 8.7, 2.5 Hz, 2H), 4.71 (d, *J* = 5.8 Hz, 2H), 3.89 (t, *J* = 7.3 Hz, 8H), 3.10 (s, 3H), 2.42 – 2.31 (m, 4H), 0.61 (s, 3H), 0.56 (s, 3H). ¹³C NMR (151 MHz, CDCl₃) δ 169.87, 167.37, 166.28, 163.80, 155.52, 150.94, 142.39, 139.34, 136.49, 131.84, 131.29, 129.17, 128.74, 128.42, 127.92, 127.70, 126.14, 122.90, 115.52, 112.45, 91.99, 52.22, 44.02, 21.21, 16.89, 0.22, -1.18. MALDI-TOF: calcd. for C₃₉H₃₈N₇O₃Si [M+H]⁺ 680.3, found 680.5.



H-Tz-Aze-SiR **11** was synthesized as described above in 65% yield. ¹H NMR (600 MHz, CDCl₃) δ 10.21 (s, 1H), 8.59 (d, *J* = 8.3 Hz, 2H), 8.04 – 7.91 (m, 2H), 7.66 (s, 1H), 7.55 (d, *J* = 8.2 Hz, 2H), 6.74 (d, *J* = 8.7 Hz, 2H), 6.64 (d, *J* = 2.5 Hz, 2H), 6.59 (t, *J* = 5.7 Hz, 1H), 6.26 (dd, *J* = 8.7, 2.5 Hz, 2H), 4.72 (d, *J* = 5.8 Hz, 2H), 3.89 (t, *J* = 7.3 Hz, 8H), 2.42 – 2.31 (m, 4H), 0.61 (s, 3H), 0.56 (s, 3H). ¹³C NMR (151 MHz, CDCl₃) δ 169.87, 166.32, 166.18, 157.86, 155.52, 150.95, 143.14, 139.31, 136.50, 132.62, 131.82, 131.03, 129.18, 128.80, 128.49, 127.93, 127.70, 126.14, 122.93, 115.52, 112.45, 92.02, 43.98, 16.88, 0.21, -1.18. MALDI-TOF: calcd. for C₃₈H₃₆N₇O₃Si [M+H]⁺ 666.3, found 666.2.

Plasmids and cloning

pCMV-HA-IFITM3 plasmid was constructed in the laboratory previously. pEF1 α -FLAG-Mm-PylRS-WT (wild-type PylRS from *Methanosarcina mazei*) and pCMV-Mm-PylRS-WT (wild-type PylRS from *Methanosarcina mazei*) were generously provided by Prof. Jason Chin at MRC Laboratory of Molecular Biology and Prof. Peng R. Chen at Peking University, respectively. pEF1 α -FLAG-Mm-PylRS-AF (Y306A and Y384F double mutant of wild-type PylRS) was generated in the lab by site-directed mutagenesis of pEF1 α -FLAG-Mm-PylRS-WT. pCMV-FLAG-Mm-PylRS-AF (Y306A and Y384F double mutant of wild-type PylRS) were also generated in the lab by site-directed mutagenesis of pCMV-Mm-PylRS-WT and introducing an in-frame N-terminal FLAG tag. FLAG-tagged Mb-BCNKRS² and Mb-TCOKRS² were synthesized by Genewiz and cloned into the pEF1 α -FLAG-Mm-PylRS-WT plasmid with NheI and BamHI in place of the wild-type Mm-PylRS-WT.

mCherry-Nucleus (Addgene plasmid # 55110), mCherry-Actin (Addgene plasmid # 54967), mCherry-Vimentin (Addgene plasmid # 55158), mCherry-Sec61 (Addgene plasmid # 55129), mCherry-GalT (Addgene plasmid # 55052), mCherry-Rab5 (Addgene plasmid # 55126), and mCherry-Rab7 (Addgene plasmid # 55127) were gifts from Prof. Michael Davidson. pLAMP1-mCherry was a gift from Prof. Amy Palmer (Addgene plasmid # 45147). HA-Actin was a gift from Prof. Alice Ting (Addgene plasmid # 34839).

TAG codons were introduced into the IFITM3 plasmid at F8 position and mCherry plasmids at I12 or Y156 position by site-directed mutagenesis. mCherry-Vimentin-N116TAG and HA-Actin-K118TAG were generated from wild-type plasmids by site-directed mutagenesis. Site-directed mutagenesis was performed with QuikChange II Site-Directed Mutagenesis Kit (Agilent) with primers designed by Agilent Primer Design Program.

Cell culture and transfection

Hela and HEK293T cells were grown in DMEM (Life Technologies) supplemented with 4.5 g/liter D-glucose, 110 mg/liter sodium pyruvate, and 10% FBS (HyClone, Thermo Scientific) at 37 °C in a humidified incubator with an atmosphere of 5% CO₂. HEK293T cells were transfected using Xtremegene 9 (Roche) with a 3:1 ratio of transfection reagent/DNA according to the manufacturer's protocol in Opti-MEM media (Life Technologies) at 70% confluence. Hela cells were transfected using Lipofectamine 3000 (Life Technologies) with a 3:1 ratio of transfection reagent/DNA according to the manufacturer's protocol in cell growth media at 80-90% confluence.

Fluorescence labeling of proteins in live cells, in-gel fluorescence, and western blotting

HEK293T or Hela cells were seeded on 12-well plates (Corning) and cultured overnight. The next day cells were co-transfected with the plasmid of interest containing a TAG codon (0.5 μ g per well) and PylRS/Pyl-tRNA plasmid (0.5 μ g per well) using 3 μ L

Xtremegene 9 or Lipofectamine 3000 in Opti-MEM media or complete cell growth media containing UAAs. After 16 h incubation, cell media were changed to fresh Opti-MEM media or complete cell growth media without UAA. After another 6 h culture at 37 °C/5% CO₂, cells were labeled with tetrazine-fluorophores (250-500 nM) in Live Cell Imaging Solution (LCIS, Life Technologies) for 0.5 h at 37 °C and then washed with Opti-MEM media or cell growth media 4 times over 2 h. After that, cells were lysed with 4% SDS lysis buffer (4% SDS, 150 mM NaCl, 50 mM triethanolamine pH 7.4, Roche protease inhibitor, benzonase) containing 100 µM bicyclo[6.1.0]non-4-yn-9-ylmethanol (SynAffix) by sonication and vortexing. The resulting cell lysates were centrifuged at 16,000 × g for 5 min at room temperature to remove cellular debris. Protein concentrations were determined by the BCA assay (Pierce).

Cell lysates were normalized by protein concentrations and diluted with 4× reducing SDS-loading buffer (40% glycerol, 200 mM Tris-HCl pH 6.8, 8% SDS, 0.4% bromophenol blue). The resulting samples were heated for 5 min at 95 °C before loaded onto 4–20% Tris-HCl gels (Bio-Rad) for SDS-PAGE separation. Generally, 20 µg of protein per gel lane is sufficient for in-gel fluorescence visualization. For in-gel fluorescence, gels were scanned on a Bio-Rad ChemiDoc MP Imager. For green tetrazine-fluorophores (fluorescein and BODIPY-FL), the fluorescein filter setting was used; for orange tetrazine-fluorophores (rhodamine), the rhodamine filter setting was used; and the Alex Fluor 647 filter setting was used for red tetrazine-fluorophores (SiR). Fluorescence intensity of every band was quantified in Image Lab (Bio-Rad). Intensity of the most intense band of each gel was set to 1 and intensities of other bands were normalized to this value. Data from three independent replicates were quantified and averaged for plotting the heat maps. After in-gel fluorescence scanning, gels were stained with Coomassie Brilliant Blue (Bio-Rad).

Another gel was loaded with identical samples as in the fluorescence gel and subjected for SDS-PAGE. Gels were transferred to nitrocellulose membranes using Bio-Rad Trans-Blot Semi-Dry Cell (20 V, 40 min), which were blocked with PBST (0.05% Tween-20 in PBS) containing 5% nonfat milk for 1 h at room temperature. The membranes were then incubated with appropriate antibodies overnight at 4 °C. Anti-HA-HRP conjugate (3F10, Roche, 1:2000 dilution) and mouse anti-RFP antibody (6G6, Chromotek, 1:1000 dilution) were used for anti-HA and anti-mCherry blots, respectively. Goat anti-mouse-HRP secondary antibody (Jackson Immunoresearch Laboratories, 1:5000 dilution) was used for mouse anti-RFP antibody in anti-mCherry blots. After overnight incubation, membranes were washed with PBST three times and developed using Bio-Rad Clarity Western ECL substrate and imaged with a Bio-Rad ChemiDoc MP Imager. Quantification of band intensities in fluorescence gels and Western blotting were performed with Image Lab (Bio-Rad).

Flow cytometry

HEK293T cells expressing GFP-Y39TAG in the presence of different UAAs were prepared as described above and then fixed with 4% formaldehyde for 15 min. After brief

washing with PBS, cells were suspended in PBS with 2% FBS and analyzed with BD LSRII Flow Cytometer.

Fixed cell imaging and immunofluorescence staining

Hela cells were seeded on coverslips in 12-well plates and cultured overnight. The next day cells were transfected with the plasmid of interest containing a TAG codon (0.5 µg per well) and PylRS/Pyl-tRNA plasmid (0.5 µg per well) using 3 µL Lipofectamine 3000 in complete cell growth media containing UAAs. After 16 h incubation, cell media were changed into fresh cell growth media without UAA. After another 6 h culture at 37 °C/5% CO₂, cells were labeled with tetrazine-fluorophores (250-500 nM) in Live Cell Imaging Solution (LCIS, Life Technologies) for 0.5 h at 37 °C and washed with cell growth media 4 times over 2 h. Then cells were fixed with 3.7% (w/v) paraformaldehyde, permeabilized with 0.1% (w/v) Triton X-100, and blocked with 5% (w/v) BSA in PBS. Cells were incubated with anti-HA-Alexa Fluor 488 or anti-HA-Alexa Fluor 594 antibody (16B12, Life Technologies, 1:250 dilution) for 30 min and washed with 0.1% (w/v) Triton X-100 three times. Finally cells were incubated with DAPI (300 nM, Life Technologies) for nucleus staining before mounting and imaging with confocal microscopy.

For immunofluorescence staining of endogenous IFITM3, Hela cells were treated with IFN-α (Cell Signaling) for 8 h after transfection. After fixation and permeabilization, cells were incubated with rabbit anti-IFITM3 antibody (Proteintech, 11714-1-AP, 1:250 dilution) for 30 min, and then with anti-rabbit-Alexa Fluor 488 conjugate (Life Technologies, 1/1,000 dilution) for another 30 min. Finally cells were incubated with DAPI (300 nM, Life Technologies) for nucleus staining before mounting and imaging with confocal microscopy.

Live cell imaging

Hela cells were seeded in 35 mm glass bottom dishes (MatTek) and cultured overnight. The next day cells were transfected with the plasmid of interest containing a TAG codon (0.7 µg per dish), PylRS/Pyl-tRNA plasmid (0.7 µg per dish) and GFP- or mCherry-LAMP1 (0.7 µg per dish) using 6 µL Lipofectamine 3000 in complete cell growth media containing UAAs. After 16 h incubation, cell media were changed into fresh cell growth media without UAA. After another 6 h culture at 37 °C/5% CO₂, cells were labeled with tetrazine-fluorophores (250-500 nM) in Live Cell Imaging Solution (LCIS, Life Technologies) for 0.5 h 37 °C and washed with FluoroBrite DMEM (Life Technologies)/10% FBS 4 times over 2 h. Finally, cells were stained with NucBlue Live Cell Stain (Life Technologies) and imaged in FluoroBrite DMEM/10% FBS with confocal microscopy.

For plasma membrane staining, cells were stained with CellMask Red (1:1000, Life Technologies) in LCIS for 5 min at 37 °C and washed with LCIS three times before staining with NucBlue Live Cell Stain. For imaging exogenous cargoes, cells were incubated with pHrodo Red-dextran (20 µg/mL, Life Technologies) or pHrodo Red-EGF (25 µg/mL, Life Technologies) in LCIS containing 1% BSA and 20 mM glucose for 30

min at 37 °C and stained with NucBlue Live Cell Stain for immediate confocal fluorescence imaging. For time-lapse imaging of dextran trafficking, cells were stained with NucBlue Live Cell Stain and plated on microscope stage maintained at 37 °C with 5% CO₂. Media were quickly removed and changed into FluoroBrite DMEM/10% FBS containing pHrodo Red-dextran (20 µg/mL, Life Technologies). Cells were then immediately monitored with confocal microscopy.

For live cell imaging of other intracellular proteins in HEK293T cells, the 35 mm glass bottom dishes were coated with poly-D-lysine (Aldrich) overnight at 4 °C and washed with PBS prior to cell seeding. HEK293T cells were transfected with the plasmid of interest containing a TAG codon (1 µg per dish) and PylRS/Pyl-tRNA plasmid (1 µg per dish) using Xtremegene 9 (6 µL per dish) in Opti-MEM media containing UAAs. After 16 h incubation, cell media were changed into fresh Opti-MEM media without UAA. After another 6 h culture at 37 °C/5% CO₂, cells were labeled with tetrazine-fluorophores (250-500 nM) in Live Cell Imaging Solution (LCIS, Life Technologies) for 0.5 h at 37 °C and washed with Opti-MEM media 4 times over 2 h. Finally, cells were stained with NucBlue Live Cell Stain and imaged in Opti-MEM media with confocal microscopy.

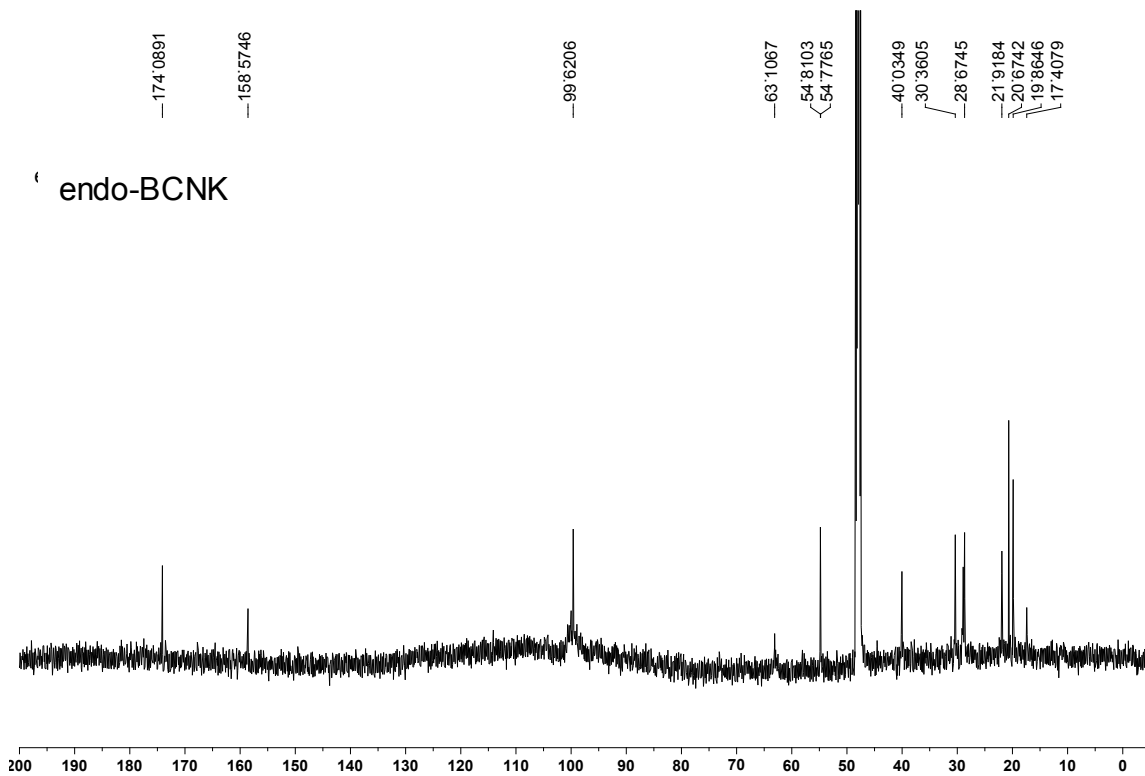
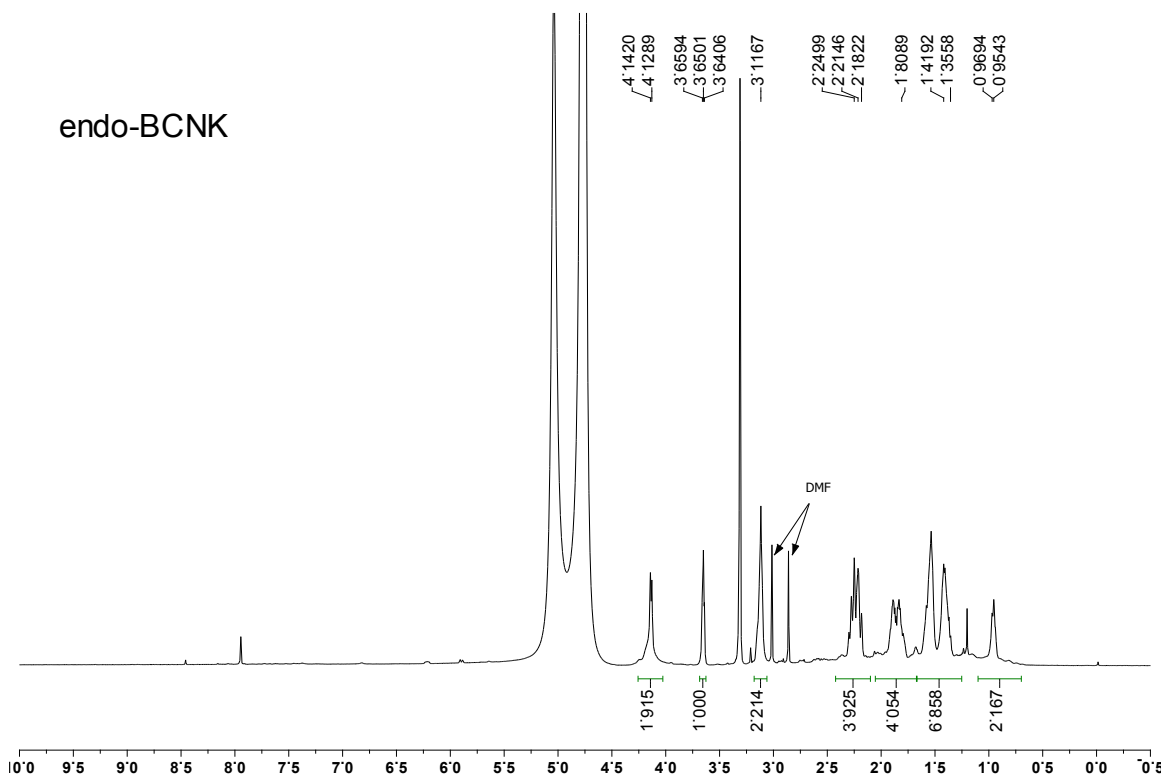
Fluorescence microscopy

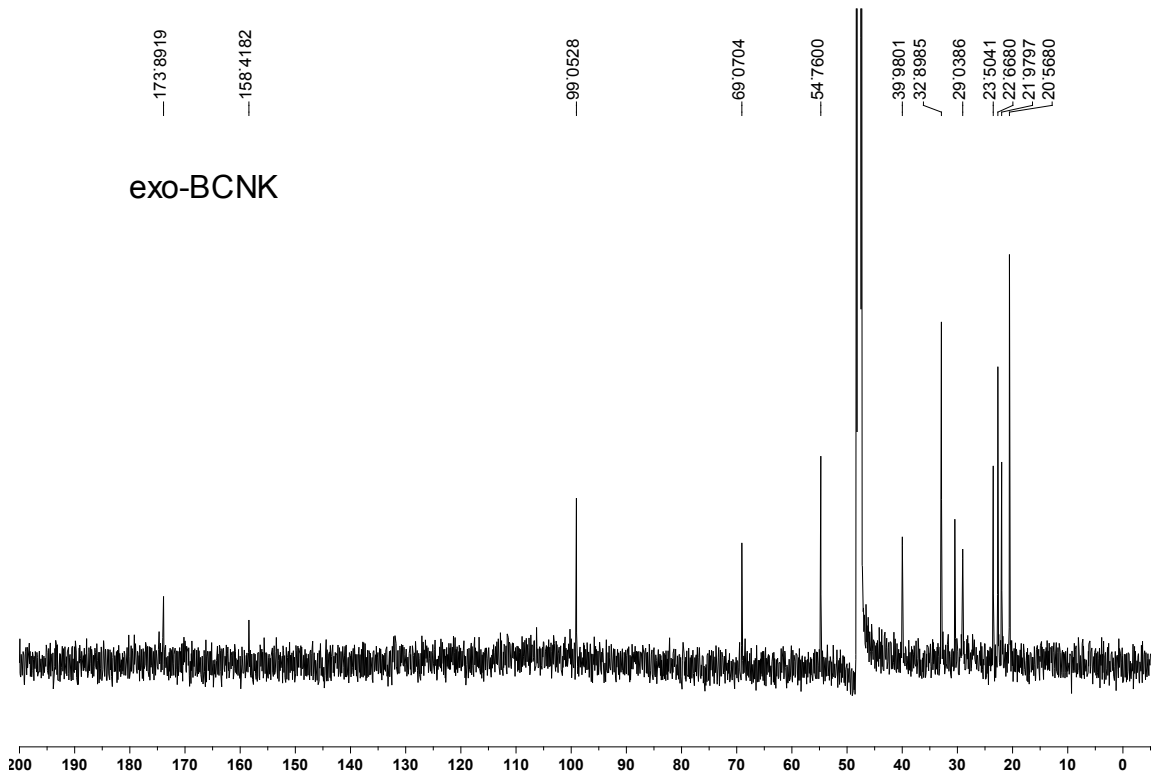
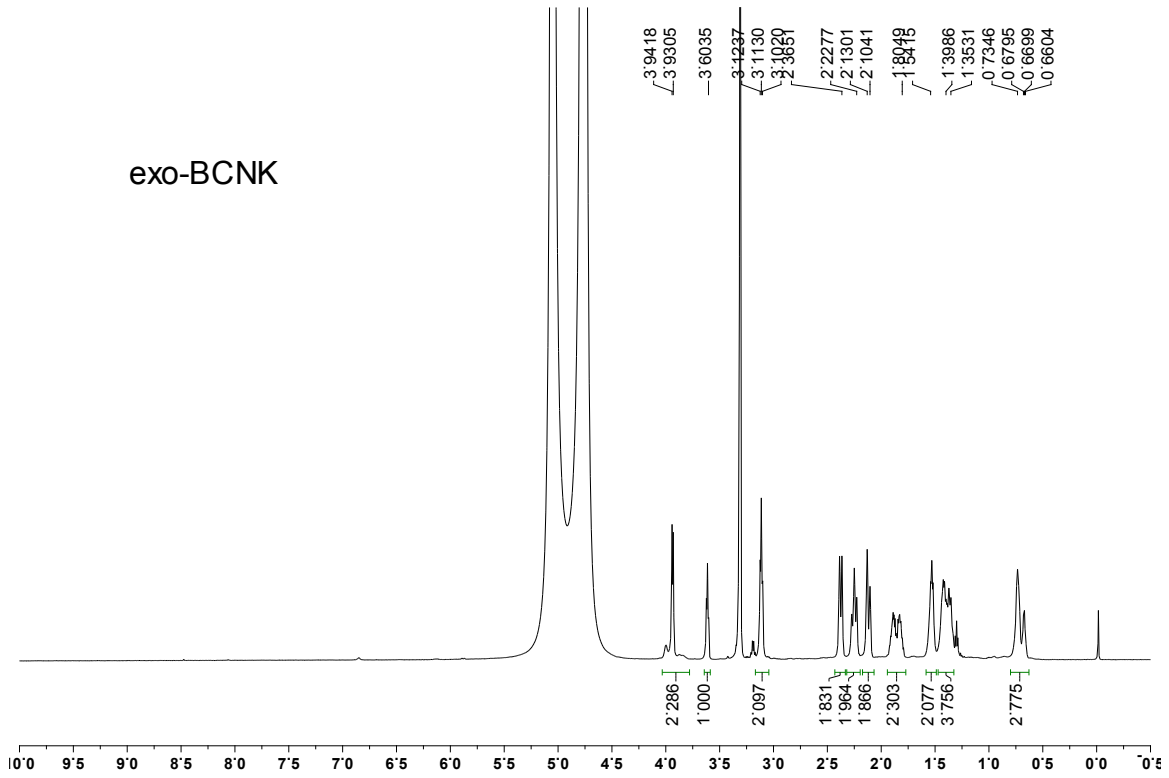
Fixed and live cells were imaged on an inverted LSM 780 laser scanning confocal microscope (Zeiss) with a Zeiss Plan-Apochromatic 63X/1.4 oil immersion objective. The microscope was equipped with a stage-top incubator set at 37 °C/5% CO₂ for live cell imaging. DAPI and Hoescht were excited with a 405 nm laser with emission spectra collected between 410 nm and 480 nm. Fluorescein, BODIPY-FL, and GFP were excited with a 488 nm laser with emission spectra collected between 490 nm and 550 nm. Rhodamine, mCherry, pHrodo Red, and CellMask Red were excited with a 561 nm laser with emission spectra collected between 570 nm and 620 nm. SiR was excited with a 633 nm laser with emission spectra collected between 650 nm and 755 nm. Images were acquired with the ZEN blue 2012 software (Zeiss) and analyzed by ImageJ (NIH). Pearson's correlation coefficients were calculated in ImageJ using the Coloc 2 plugin. For time-lapse imaging, images were acquired every 30 s with Definite Focus activated to correct focus drift.

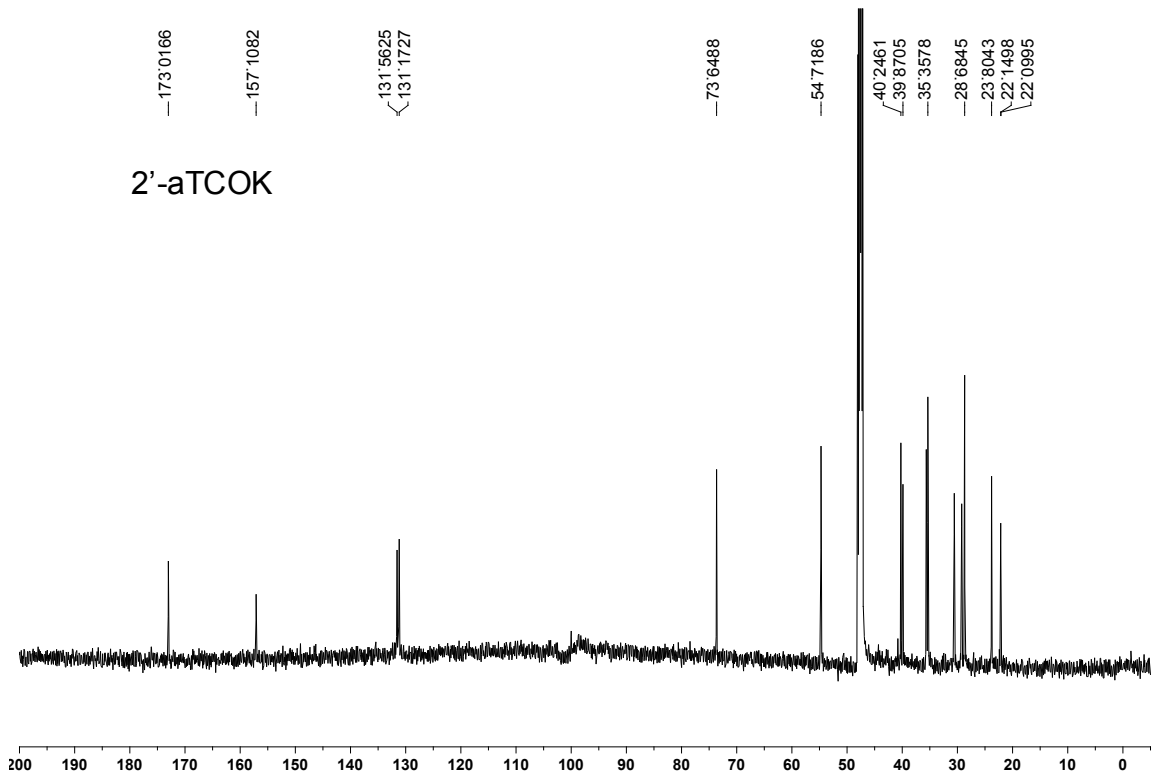
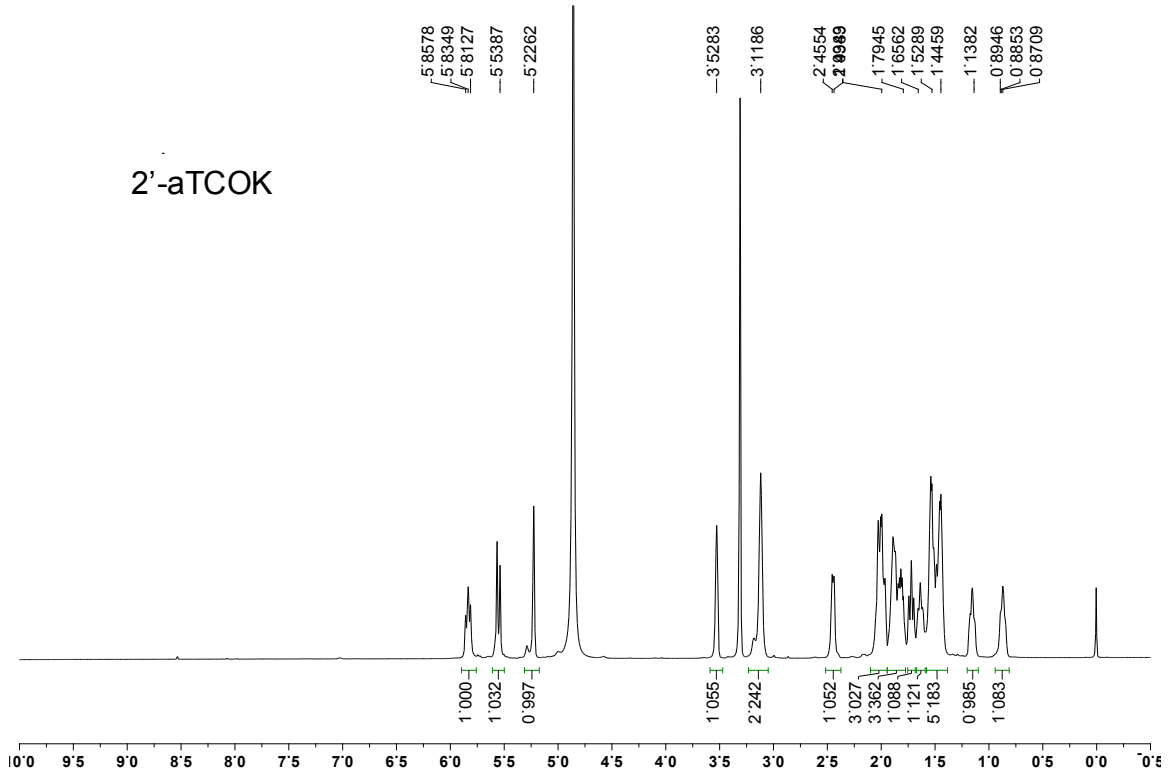
References:

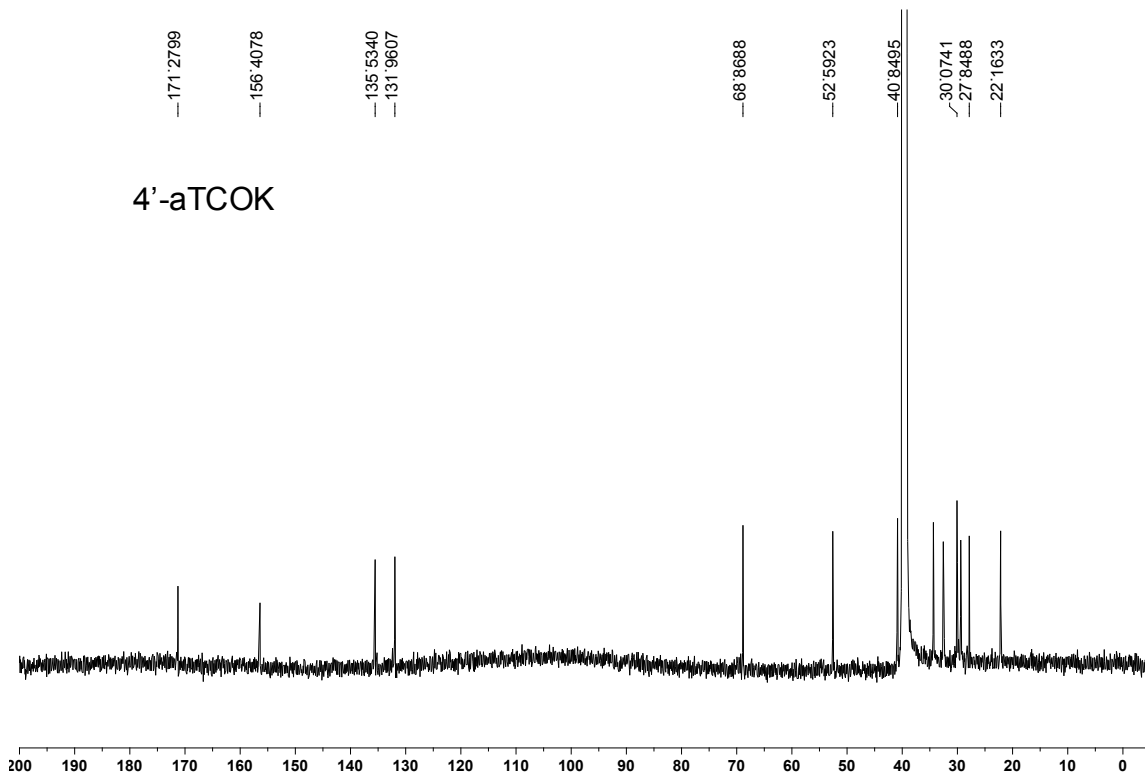
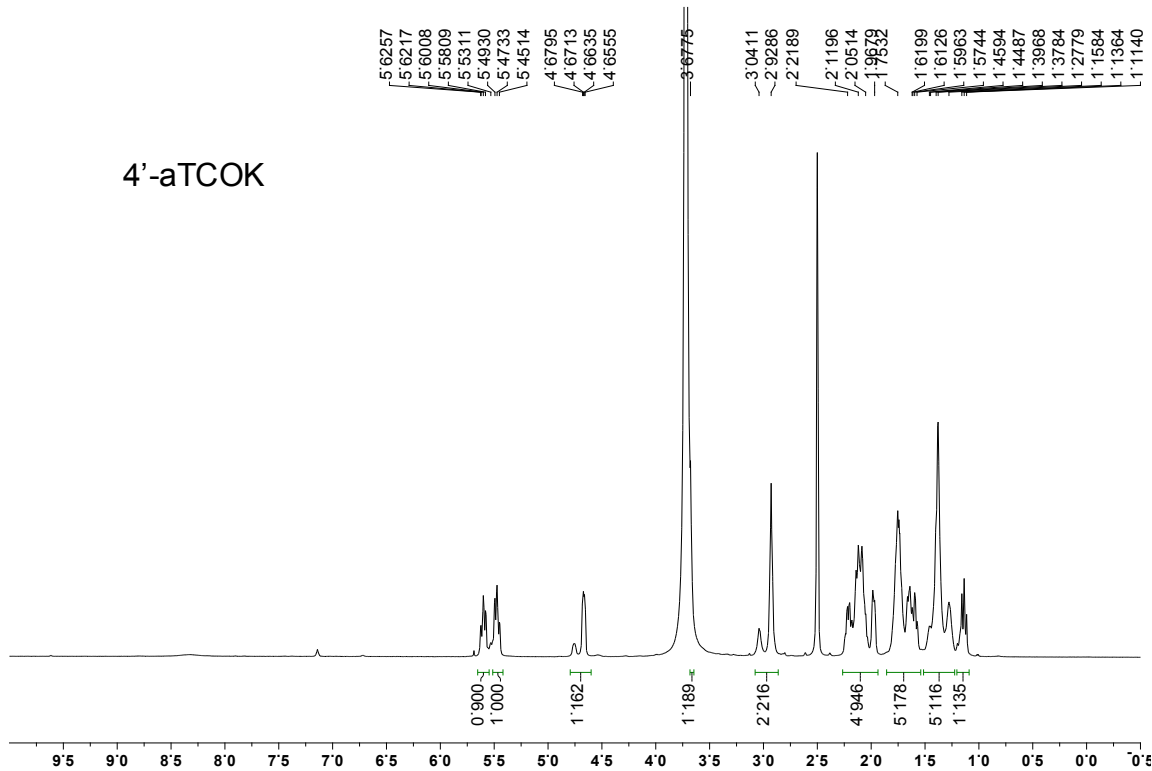
- (1) Schmied, W. H.; Elsässer, S. J.; Uttamapinant, C.; Chin, J. W. *J. Am. Chem. Soc.* **2014**, *136*, 15577.
- (2) Lang, K.; Davis, L.; Wallace, S.; Mahesh, M.; Cox, D. J.; Blackman, M. L.; Fox, J. M.; Chin, J. W. *J. Am. Chem. Soc.* **2012**, *134*, 10317.
- (3) Li, J.; Yu, J.; Zhao, J.; Wang, J.; Zheng, S.; Lin, S.; Chen, L.; Yang, M.; Jia, S.; Zhang, X.; Chen, P. R. *Nat. Chem.* **2014**, *6*, 352.
- (4) Yount, J. S.; Karssemeijer, R. A.; Hang, H. C. *J. Biol. Chem.* **2012**, *287*, 19631.
- (5) Elliott, T. S.; Townsley, F. M.; Bianco, A.; Ernst, R. J.; Sachdeva, A.; Elsasser, S. J.; Davis, L.; Lang, K.; Pisa, R.; Greiss, S.; Lilley, K. S.; Chin, J. W. *Nat. Biotech.* **2014**, *32*, 465.
- (6) Li, J.; Jia, S.; Chen, P. R. *Nat. Chem. Biol.* **2014**, *10*, 1003.
- (7) Carlson, J. C. T.; Meimetis, L. G.; Hilderbrand, S. A.; Weissleder, R. *Angew. Chem., Int. Ed.* **2013**, *52*, 6917.
- (8) Lukinavičius, G.; Umezawa, K.; Olivier, N.; Honigmann, A.; Yang, G.; Plass, T.; Mueller, V.; Reymond, L.; Corrêa Jr, I. R.; Luo, Z.-G.; Schultz, C.; Lemke, E. A.; Heppenstall, P.; Eggeling, C.; Manley, S.; Johnsson, K. *Nat. Chem.* **2013**, *5*, 132.
- (9) Grimm, J. B.; English, B. P.; Chen, J.; Slaughter, J. P.; Zhang, Z.; Revyakin, A.; Patel, R.; Macklin, J. J.; Normanno, D.; Singer, R. H.; Lionnet, T.; Lavis, L. D. *Nat. Meth.* **2015**, *12*, 244.
- (10) Karver, M. R.; Weissleder, R.; Hilderbrand, S. A. *Bioconjugate Chem.* **2011**, *22*, 2263.
- (11) Yang, K. S.; Budin, G.; Reiner, T.; Vinegoni, C.; Weissleder, R. *Angew. Chem., Int. Ed.* **2012**, *51*, 6598.
- (12) Devaraj, N. K.; Hilderbrand, S.; Upadhyay, R.; Mazitschek, R.; Weissleder, R. *Angew. Chem., Int. Ed.* **2010**, *49*, 2869.
- (13) Liu, D. S.; Tangpeerachaikul, A.; Selvaraj, R.; Taylor, M. T.; Fox, J. M.; Ting, A. Y. *J. Am. Chem. Soc.* **2012**, *134*, 792.
- (14) Erdmann, R. S.; Takakura, H.; Thompson, A. D.; Rivera-Molina, F.; Allgeyer, E. S.; Bewersdorf, J.; Toomre, D.; Schepartz, A. *Angew. Chem., Int. Ed.* **2014**, *53*, 10242.

NMR

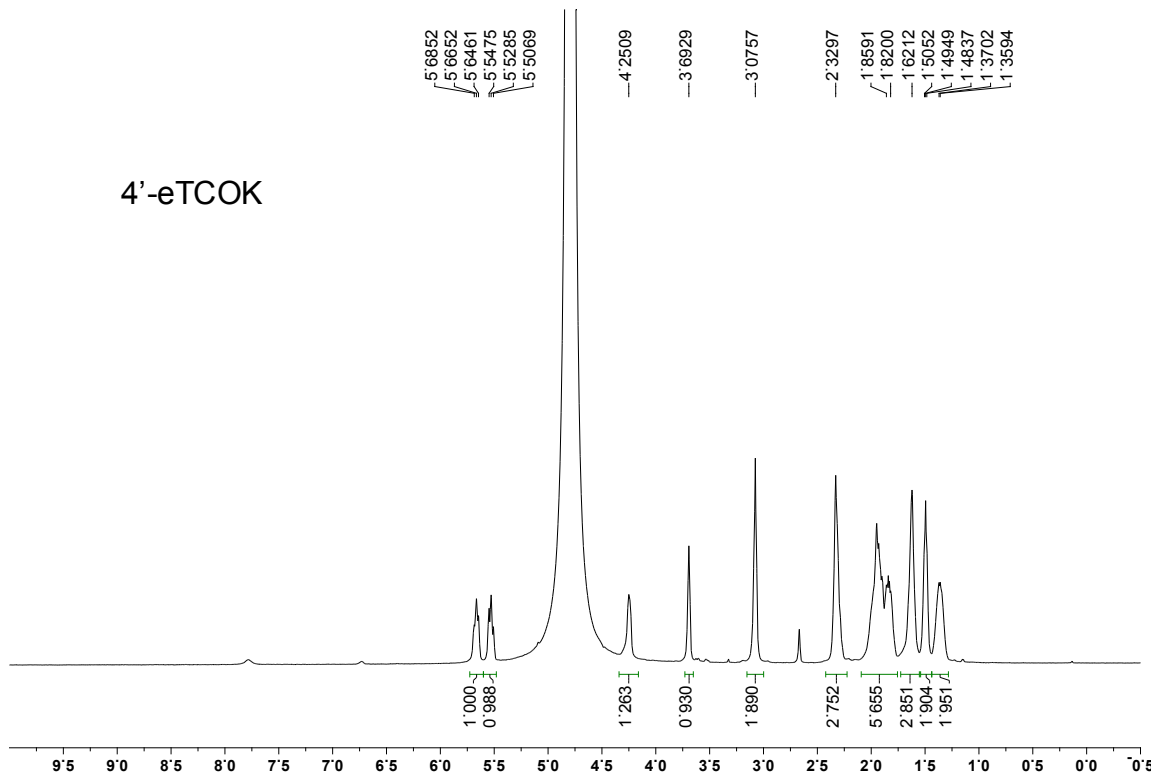








4'-eTCOK



4'-eTCOK

